NATIONAL ADVISORY COMMITTEE FOR AERONAUTICS

TECHNICAL NOTE 1904

OBSERVATIONS OF ICING CONDITIONS ENCOUNTERED IN FLIGHT DURING 1948

By William Lewis and Walter H. Hoecker, Jr.

Ames Aeronautical Laboratory
Moffett Field, Calif.

Washington
June 1949

NATIONAL ADVISORY COMMITTEE FOR AERONAUTICS

TECHNICAL NOTE 1904

OBSERVATIONS OF ICING CONDITIONS ENCOUNTERED IN FLIGHT DURING 1948

By William Lewis[1] and Walter H. Hoecker, Jr.[1]

SUMMARY

Meteorological data from flight observations in icing conditions during the first 5 months of 1948 are presented. A total of 335 measurements of liquid-water content and mean-effective drop diameter were obtained by the multicylinder method in the course of 40 flights in icing conditions covering most of northern United States. Cumulus clouds were predominant during approximately two-thirds of the flights. A continuous record of liquid-water content covering a major portion of the operations was obtained by means of a rotating-disk icing-rate meter. This record was used to investigate the relation between average liquid-water content and the horizontal extent of icing conditions. An analysis of values of maximum drop diameter calculated from the area of drop impingement on a stationary cylinder and corresponding values of mean-effective drop diameter and drop-size distribution as obtained from the rotating cylinders led to the conclusion that the rotating-cylinder indications of drop-size distribution are so unreliable that they are of little or no value. The data indicate that average and maximum values of drop size are significantly greater and more variable near the Pacific coast than in the other parts of the United States included in this investigation.

INTRODUCTION

A considerable amount of data on the physical characteristics of natural icing conditions has been obtained in flight as part of the ice-prevention research program conducted by the Ames Aeronautical Laboratory of the NACA. The meteorological results of this program

---

[1]U. S. Weather Bureau meteorologists assigned to collaborate with the Ames Aeronautical Laboratory on icing research.

up to and including the 1946-47 season have been presented in references 1 and 2. This report presents the results of additional observations made during the first 5 months of 1948.

The object of all of these observations has been to establish, for the pertinent meteorological variables, the range of values commonly encountered in icing conditions. These data are required as a basis for the definition of the physical characteristics of the maximum icing conditions in which ice-prevention equipment will be expected to provide adequate protection. Tentative estimates of maximum icing conditions have been proposed in references 1 and 2. These estimates have been re-examined in the light of the additional data obtained during 1948, with consideration also being given to available data from other sources, and a revised and extended listing of conditions recommended for consideration in the design of ice-protection equipment has been prepared (reference 3). Since the data presented herein were considered in the preparation of reference 3, specific recommendations for design values are not included in this report.

In addition to the presentation of the detailed results of the 1948 observations, this report includes a discussion of the relation between the extent of icing conditions and the average liquid-water content observed in them, the reliability of measurements of drop-size distribution, and an apparent geographical influence upon the size of cloud drops.

Appreciation is extended to the Air Materiel Command of the U. S. Air Force and to the U. S. Weather Bureau for cooperation in the research program.

APPARATUS AND METHOD

The airplane used in this investigation was a twin-engine transport equipped with a thermal ice-prevention system which previous flight experience had shown to provide satisfactory protection in severe icing conditions (reference 4).

The following apparatus and instruments for the measurement of the meteorological factors pertaining to icing were installed in the airplane for the 1948 season:

1. Airspeed indicator and altimeter

2. NACA airspeed and altitude recorder

3. Thermocouple shielded against the accretion of ice, and millivoltmeter for measurement of free-air temperature

4. Rotating multicylinders for the determination of liquid-water content and mean-effective drop size[2]

5. Cloud indicator

6. Fixed cylinder for determination of maximum drop size

7. Rotating-disk icing-rate meter

Items 1 and 2 are standard instruments and need not be described here. Item 3 was discussed in reference 1, and item 4 in reference 2. Items 5, 6, and 7 are discussed in the appendix of this report.

RESULTS

The basic data obtained by the rotating-multicylinder method are presented in table I in a form similar to that used in reference 2. Two values of liquid-water content are included in the table. The first, w_1, is the average over the total time during which the rotating cylinders were exposed. The second, w_2, is the average over that portion of the cylinder exposure period during which the presence of liquid cloud drops was indicated by the cloud indicator. The quantity w_2 thus includes a correction for areas of clear air or dry snow within or between cloud masses. The quantity w_1 is comparable with values of liquid-water content reported for previous seasons. Values of maximum drop diameter obtained from the fixed-cylinder observations are also included in table I.

In addition to the rotating-cylinder observations, a continuous record of liquid-water content encountered during a major part of the season's operations is available from the rotating-disk records. These data are presented in terms of icing instances, defined as periods of continuous icing as indicated by the instrument. Since the reading of the icing-rate meter represents the average liquid-water content over a period of about 10 seconds, breaks in a cloud which required less than 10 seconds to traverse (horizontal extent of 1/2 mile at 180 mph) are included in periods of continuous icing recorded in this way. Hence, an icing instance as defined above is a period of icing, including breaks of 10 seconds or less, which was preceded and followed by intervals of

[2]The amount of water in all of the drops of a diameter greater than the mean-effective diameter is equal to the amount of water in all of the drops of smaller diameter.

more than 10 seconds during which the liquid-water content was zero. In most cases this represents a single run through a continuous or nearly continuous cloud, although at times several turns were made within a single cloud with the result that the indicated duration of the icing instance was occasionally as much as three or four times as long as the time required for a single straight flight through the cloud.

The records of the icing-rate meter were used to determine the greatest average liquid-water content for each flight, averaged over the following elapsed time intervals: 10 seconds, 1 minute, 5 minutes, and 20 minutes, which correspond approximately to horizontal distances of 1/2, 3, 15, and 60 miles, respectively, since the average flight speed was 180 miles per hour.

These results and a summary of the data in terms of icing instances are presented in table II.

The records obtained with the cloud indicator, supplemented by visual observations of the presence or absence of snow in the air, were used to prepare table III which presents the frequency of encounter of various meteorological conditions classified according to the type of water particles present. The table includes a summation of the prevailing conditions during each minute of flight from take-off to landing during daylight hours on flights in which icing conditions, clouds, or precipitation were encountered. Percentages are given based on total time covered by the tabulation and also the time during which visible moisture was present.

Since this tabulation is based on a time interval of 1 minute at an average flight speed of 180 miles per hour, conditions listed as continuous represent unbroken cloud masses extending for more than 3 miles along the flight path.

DISCUSSION

The manner in which the investigation of meteorological conditions was conducted during the 1948 season differed from that of previous seasons in three important respects: First, a larger percentage of the flights were made in cumulus clouds; second, a larger proportion of the flights were made along the Pacific coast; and, third, the average altitude was higher and the average temperature was lower. These differences, which were due mainly to an attempt to operate as much as possible at low temperatures for the study of propeller icing, should be considered when the data herein are compared with those from previous seasons.

The flights reported herein also included the only encounter with freezing rain in 4 successive years of this type of operation. Unfortunately, on this occasion, the intensity of the rain was so light that the water content of the rain could not be measured in the presence of the clouds through which it was falling. The total liquid-water content of rain and cloud was 0.08 to 0.09 gram per cubic meter, and the mean-effective drop diameter of the mixture as measured by the rotating cylinders was 18 to 20 microns. The maximum impingement angle on the fixed cylinder was 90°, indicating a maximum drop diameter of over 150 microns. The temperature was 26° F to 28° F, and, as the flight continued in the direction of lower temperatures, the airplane passed from freezing rain to snow at 25° F.

The Discontinuous Character of Icing Clouds

The data in table III show the comparative scarcity of continuous icing clouds. As shown in the last column of table III, 5.0 percent of the time in continuous or intermittent clouds or precipitation was in continuous clouds of liquid drops and 4.3 percent was in continuous clouds of mixed composition with liquid drops predominating, making a total of only 9.3 percent in continuous clouds of a type in which appreciable icing is likely. An examination of table III also reveals that the relative frequency of continuous and discontinuous clouds depends upon the cloud composition. The following table shows, for each type of cloud composition, the percentage of time in continuous and discontinuous clouds:

Cloud composition	Percentage continuous	Percentage discontinuous
Liquid drops	15	85
Mixed, liquid predominant	32	68
Mixed, snow predominant	74	26
Snow	83	17

These results show that clouds in which liquid drops predominate are typically discontinuous, while clouds composed mostly of snow are usually more continuous.

Additional information concerning the discontinuous character of icing conditions may be obtained from the records of the rotating-disk icing-rate meter. Frequency distributions of the duration of icing instances, defined as periods of continuous icing as recorded by the icing-rate meter, are presented in figure 1. In this figure, curve A shows the relative frequency of observations of various values of duration of icing instances. Curve B represents the percentage of the total time in icing conditions which was included in icing instances of less than a given duration. It should be noted that the durations of icing instances, as determined with the icing-rate meter, are approximately 10 seconds greater than the actual time in clouds due to the averaging characteristics of the instrument. (See appendix.)

It is seen from an examination of curve A, figure 1, that, for example, 90 percent of the icing instances were less than 2.5 minutes in duration and 67 percent less than 1 minute. Curve B shows that 50 percent of the time in measurable icing was included in instances of less than 2 minutes duration and slightly less than 10 percent in instances longer than 7 minutes.

Variation of Average Liquid-Water Content With Extent of Icing Conditions

Since the harmful effects of an encounter with icing conditions depend on the extent as well as the intensity of the conditions, the discontinuous character of icing clouds is an important factor to be considered in the design of ice-protection equipment. In this connection it is desirable to determine, for any given number of icing flights, the most probable maximum values of liquid-water content averaged over various distances along the flight path. The continuous records of liquid-water content obtained with the icing-rate meter provide the data required for a tentative solution of this problem.

Statistical analysis of the icing-rate meter records.- The data in table II include, for each flight, the greatest average liquid-water content averaged over elapsed time intervals of 10 seconds, 1 minute, 5 minutes, and 20 minutes. At 180 miles per hour, which was the approximate average flight speed of the test airplane, these time intervals correspond to distances along the flight path of 1/2, 3, 15, and 60 miles. Frequency distributions of each of these quantities are shown in figure 2 for layer clouds and cumulus clouds. The arithmetical-mean values of maximum liquid-water content for the intervals listed above are 1.05, 0.63, 0.33, and 0.14 grams per cubic meter, respectively, for cumulus clouds and 0.44, 0.27, 0.16, and 0.08 for layer clouds. These values decrease steadily for longer time intervals as would be expected.

These frequency distributions can be used to determine roughly the maximum values of water content to be expected in the course of a given number of icing flights. If data were available from a very large number of flights in icing conditions, n, during which a value of liquid-water content, w, was reached or exceeded m times, then a liquid-water content of w or more would be expected to occur once in $n/m = N$ flights and the probability, P, of encountering a liquid-water content of w or more on any one flight is $P = 1/N$. If N is plotted against w, a curve is obtained which indicates the greatest value of liquid-water content to be expected in any number of flights.

Since data are available for only a small number of flights ($n = 26$ for cumulus clouds and $n = 11$ for layer clouds), some reliable means of smoothing and extrapolating the curve relating w and N is desirable. For this purpose, a mathematical expression for the frequency distribution of the maximum values of liquid-water content is required. Such an expression has been found by Gumbel (reference 5) which closely approximates the observed distributions of maximum values of several meteorological quantities. This distribution is of the form,

$$1-P = \exp.\left[-e^{-a(x-u)}\right]$$

where a and u are constants which can be determined from the mean and the standard deviation. Distribution curves determined by this equation are included in figure 2 for comparison with the observed distributions.

Figure 3 shows w as a function of N for the calculated distributions with points determined from the observed data and the equation $N = n/m$ included for comparison. These curves indicate, for various elapsed time intervals, the maximum values of average liquid-water content that can reasonably be expected to be encountered in any given number of flights in icing conditions.

It must be emphasized that, due to the small number of cases included in the analysis, the results are not quantitatively accurate. They do, however, give a general idea of the relation between extent and average liquid-water content in icing conditions. Another important factor which affects the validity of these results is the effect of the circling flight paths which were followed in an effort to remain in cumulus clouds. The actual horizontal extent of most of the cumulus clouds investigated was from 1 to 3 miles. The high values of water content recorded for longer distances were due to the practice of circling within clouds or making repeated passes through a single cloud. For this reason, the frequency data for 10 seconds duration (1/2 mile) in cumulus clouds are regarded as representative, the values for 1 minute (3 miles) are subject to some error, but are regarded as approximately representative, while the results for 5 minutes (15 miles) or more are believed to be considerably higher than would be encountered in straight flight.

Data from figure 3 have been replotted in figure 4 to show the relation between horizontal extent and maximum average liquid-water content. The curves represent, for various distances along the flight path, the values of average liquid-water content likely to be exceeded once in 2, 10, 100 and 1000 flights in which icing conditions are encountered.

<u>Comparison with data from previous seasons</u>.- The data from previous seasons (references 1 and 2) have been used to calculate the distribution of maximum liquid-water content per icing flight for cumulus clouds and layer clouds using the method of reference 5. These data consist of rotating-cylinder measurements having an average duration of approximately 1 minute in cumulus clouds and a little over 3 minutes in layer clouds. The results of these calculations are given in the following table:

Maximum Liquid-Water Content To Be Expected (expressed as an average for the distances indicated, as a function of the number of flights in icing conditions)		
No. of flights in icing conditions	Max. av. liquid-water content to be expected over any 3-mile distance in cumulus clouds (values based on 21 flights) (g/m^3)	Max. av. liquid-water content to be expected over any 10-mile distance in layer clouds (values based on 51 flights) (g/m^3)
2	0.65	0.27
10	1.18	.43
100	1.86	.68
950	– – –	.91
1000	2.5	.92

These results have been plotted in figure 4 for comparison with the 1948 data. It is noted that the agreement is very good for the cumulus clouds, but that the conditions encountered in layer clouds during 1948 were considerably milder than those observed previously. This difference is probably due to the fact that the layer clouds investigated this season were mostly of the altocumulus type, while stratocumulus clouds predominated in the 1945-46 and 1946-47 investigations. This difference in prevailing cloud type is illustrated by the fact that the average altitude and temperature in layer clouds for the 1948 season were 11,000 feet and 13° F as compared with 5,600 feet and 16° F for the previous two seasons.

Estimated maximum liquid-water content for 1000 flights in icing conditions.- The application of the data included in figure 4 to the problems of the design of ice-prevention equipment is complicated by three factors: (1) The data for cumulus clouds are representative only for values of extent of 3 miles or less; (2) the data for layer clouds include only a very small number of flights which were made mainly in altocumulus clouds in which the water content is low compared to conditions in stratocumulus clouds; and (3) since the relative frequency of encounters with icing in cumulus and layer clouds depends to a great extent on flight procedures, the data from this investigation are not representative of normal airplane operation in this respect.

In spite of these difficulties, an attempt can be made to estimate the relation between maximum liquid-water content and the horizontal extent of icing conditions as they would normally be encountered. This estimate is based upon the following assumptions: (1) That 5 percent of the icing encounters occur in cumulus clouds;[3] (2) that the data of figure 4 are representative for cumulus clouds up to 3 miles in extent; (3) that the data from references 1 and 2 for layer clouds are representative of stratocumulus and altocumulus clouds in about the proportion normally encountered, and that the maximum values as measured by means of the rotating cylinders represent conditions 10 miles in extent; and (4) that the curves for layer clouds in figure 4(b) correctly represent the percentage variations of liquid-water content with extent in layer clouds in general.

On the basis of these assumptions, the curve presented in figure 5 has been constructed to represent the maximum average values of liquid-water content to be expected in the course of 1000 encounters with icing conditions, including 50 cases of cumulus clouds and 950 cases of layer clouds. The portion of the curve representing conditions 3 miles or less in extent gives the maximum liquid-water content to be expected in 50 encounters with cumulus clouds, based on the data in figure 4(a). The value, 0.91 gram per cubic meter for an extent of 10 miles, is expected to occur once in 950 flights in layer clouds, as shown in the foregoing table based on the data of 1945 to 1947. The portion of the curve defining conditions more than 10 miles in extent was drawn from this point parallel to the curve in figure 4(b)

[3]This estimate is based on German experience reported in reference 6.

representing the 1000-flight maximum for layer clouds. The portion of the curve between 3 miles and 10 miles was interpolated. Specific values obtained from the curve in figure 5 are presented in the following table:

Distance along flight path (miles)	Maximum average liquid-water content (g/m^3)
0.5	2.2
1.0	1.9
2.5	1.6
5	1.2
10	.9
25	.7
60	.5

The Variation of Drop Diameter From Year to Year and With Geographic Location

The most obvious difference between the data presented herein and those obtained in previous years (references 1 and 2) is in the average drop size observed. The median of all observations of mean-effective diameter for this season was 20 microns as compared with 13 microns in 1946-47 and 14 microns in 1945-46. In order to determine whether this difference could be explained on the basis of geographic location and cloud type, the average drop diameter and the standard deviation of drop diameter were calculated for layer clouds and cumulus clouds for each of three areas defined as follows: (1) The Pacific coast region, including the area west of a line about 100 miles east of the Sierra Nevada and Cascade ranges; (2) the Plateau region, extending eastward from the line just defined and including the Rocky Mountain area; and (3) eastern United States, including the Great Plains and extending eastward to the Atlantic coast. The results of this classification of drop-size data are shown in the following table in which data were included only for categories in which 20 or more observations were available.

Season	Item	Pacific Coast		Plateau		East	
		Cumulus	Layer cloud	Cumulus	Layer cloud	Cumulus	Layer cloud
1945–46	Av. diam. (microns)	16.5	16.5	17.9	10.8	---	---
	Std.deviation (microns)	5.6	9.6	4.2	3.5	---	---
	No. of observations	78	34	23	61	---	---
1946–47	Av. diam. (microns)	---	---	---	---	---	13.4
	Std.deviation (microns)	---	---	---	---	---	4.9
	No. of observations	---	---	---	---	---	112
1948	Av. diam. (microns)	23.6	20.3	---	---	18.6	14.1
	Std.deviation (microns)	7.6	7.7	---	---	5.7	5.1
	No. of observations	142	62	---	---	43	63

This table contains sufficient data for a comparison of seasonal averages for only three cases, Pacific coast cumulus and layer clouds, and Eastern layer clouds. The data for layer clouds in eastern United States show only a slight, and probably insignificant, difference between the 1946–47 and 1948 averages. In the Pacific coast observations, on the other hand, there is a significant difference between the 1945–46 and 1948 observations.

The difference may be due to: (1) different methods of measurement, since most of the 1945–46 observations were made with only two cylinders while four were used for all of the 1948 measurements; (2) differences of altitude and temperature, since the average altitude was higher and the average temperature was lower for the 1948 observations; or (3) real variations in average drop size from year to year as a result of differences in prevailing air-mass characteristics. It is believed that, over the prevailing range of drop diameters, the errors in the two-cylinder observations would be distributed in such a way as to tend to increase rather than decrease the average value, since large positive errors are more likely than large negative errors.

Hence, the observed difference in yearly average is not likely to be due to different methods of measurement. As indicated in reference 1, no significant relationship between drop size and temperature or altitude could be found in the 1945–46 data. As a further check of the possibility that the differences in drop size were due to altitude or temperature effects, the 1948 data for cumulus clouds in the Pacific coast region were used to determine correlation coefficients for the relation between drop diameter and both temperature and altitude. The correlation coefficients were –0.04 between drop diameter and temperature and 0.14 between drop diameter and altitude. These low correlation coefficients indicate that drop size is practically independent of altitude and temperature in Pacific coast cumulus clouds. It appears likely, therefore, that real variations in average drop size occur from year to year, at least in the Pacific coast region.

It is also noted that the average drop diameter for the Pacific coast area is significantly greater than for the Eastern section. The diameters are also more variable in the Pacific coast region as shown by the greater values of standard deviation. These facts suggest that the existence of large cloud drops may be regarded as a climatic characteristic of the Pacific coast region in winter which may possibly be related to the prevalence of unstable, polar-maritime air containing an unusually small concentration of condensation nuclei.

Drop-Size Distribution Measurement

The use of the rotating cylinders and the fixed cylinder for the measurement of drop sizes yields values of three quantities; namely, mean-effective diameter, maximum diameter, and distribution of drop diameters. If these data are mutually consistent, the ratio γ of the maximum diameter to the mean-effective diameter should be significantly greater for cases in which an E distribution[4] is obtained than for an A distribution. In the E distribution, as defined in reference 7, 15 percent of the liquid water is contained in drops of at least twice the mean-effective diameter. It is thus reasonable to expect the average value of γ to be in the neighborhood of 2 for an E distribution. Since the drop size is uniform for the A distribution, the average value of γ would be expected to be 1.0 for this case. The following table contains frequency distributions of γ

[4] The rotating-cylinder method gives drop-size distribution in terms of the scale defined in reference 7 in which A represents uniform drop size and B, C, D, and E represent increasing degrees of nonuniformity.

for cases in which the drop-size distribution indicated by the rotating-cylinder data was A and E. Since relative differences in γ are more significant in this case than absolute values, the group limits for the frequency table were chosen to correspond to equal intervals of log γ.

γ	A distribution (percentage based on 162 cases)	E distribution (percentage based on 61 cases)
Less than 0.45	0	3.3
0.45 to 0.56	0	1.6
0.56 to 0.71	2.5	3.3
0.71 to 0.89	11.7	29.5
0.89 to 1.12	42.0	29.5
1.12 to 1.41	23.5	14.8
1.41 to 1.78	11.7	8.2
1.78 to 2.24	4.3	3.3
Over 2.24	4.3	6.5

The results for the A distribution show a maximum frequency of γ near 1.0, which was to be expected. In the case of the E distribution, however, the most frequent value of γ was a little less than 1.0; whereas the value expected on the basis of the definition of the E distribution was about 2. The data on mean-effective diameter, maximum diameter, and diameter distribution are therefore inconsistent.

This inconsistency must be due to errors in the measurement of one or more of the quantities involved. One means of determining which of the quantities is most likely to be in error is by an examination of various possible hypotheses. First, if it is assumed that the rotating-cylinder measurements of mean-effective diameter and diameter distribution are correct, the error must be in the measurements of maximum diameter. The observed distribution of values of γ for the A drop-size distributions could be adequately explained on this basis, since it would require an approximately random distribution of errors in maximum diameter with a moderate preponderance of positive errors. However, the observed distribution of γ for the E drop-size distribution would require a peculiar distribution of error in maximum diameter with a very strong preponderance of negative errors of just the right magnitude to make γ fall between 0.7 and 1.1. Since it is reasonable to assume that such a distribution of errors in maximum diameter is highly unlikely to occur, the hypothesis that the chief source of the discrepancy is error in measurement of maximum diameter must be rejected.

A second possible assumption that the chief source of the discrepancy lies in errors in the measurement of mean-effective diameter leads to similar conclusions. This assumption could also be rejected on the basis of the fact that errors in weight of ice collected on the rotating cylinders of a sufficient magnitude to produce large errors in mean-effective diameter would be almost certain to produce large errors in drop-size distribution.

The third alternative is that the principal source of error is in the determination of drop-size distribution by means of the rotating cylinders. This appears to be the most reasonable hypothesis since the most frequent value of γ is near unity for both indicated size distributions. It is reasonable to conclude, therefore, that the drop-size distributions ordinarily encountered in clouds are usually nearly uniform and that the indications of other types of distribution by the rotating-cylinder method are unreliable.

On the basis of these considerations, it is reasonable to infer that values of mean-effective diameter associated with indicated A distributions are more reliable than those associated with indicated E distributions since the indication of an E distribution usually results from errors in the rotating-cylinder data. This accounts for the greater dispersion of values of γ for the E distribution.

On the basis of these results, it is believed that measurements of drop-size distribution made in flight by the rotating-cylinder method, including those presented in table I, are so unreliable that they are of little or no value.

CONCLUSIONS

The following conclusions are drawn from an analysis of flight data presented herein and in previous reports:

1. An analysis of continuous records of liquid-water content obtained with the rotating-disk icing-rate meter, adjusted by comparison with rotating-cylinder data from previous seasons, yields the following values of maximum liquid-water content averaged over various distances. These values are likely to be encountered once in the course of 1000 flights in icing conditions when it is assumed that 5 percent of the flights encounter cumulus clouds.

Distance along flight path, (miles)	Maximum average liquid-water content (g/m³)
0.5	2.2
1.0	1.9
2.5	1.6
5	1.2
10	.9
25	.7
60	.5

2. Average and maximum values of cloud-drop diameter are significantly larger and more variable near the Pacific coast than in other parts of the United States included in this investigation.

3. A comparison of data on drop-size distribution obtained by the rotating-cylinder method with values of maximum drop diameter as determined from the area of impingement on a stationary cylinder indicates that measurements of drop-size distribution made in flight by the rotating-cylinder method, including those presented herein, are so unreliable that they are of little or no value.

Ames Aeronautical Laboratory,
National Advisory Committee for Aeronautics,
Moffett Field, Calif.

APPENDIX

THE CLOUD INDICATOR

It had become apparent during previous years that an instrumental method of supplementing visual observations of the time of entering and leaving clouds, and the patchy or uniform characteristics of the cloud masses was desirable. The cloud indicator was designed to meet this need. This instrument consists of a heated cylinder 5/8 inch in diameter exposed at right angles to the air stream, with a thermocouple installed to measure the surface temperature at the stagnation point. To provide a continuous surface-temperature record, the thermocouple is connected to a self-balancing potentiometer equipped to provide a continuous ink trace of the variations in temperature. In use, the heating power supplied to the cylinder is adjusted to maintain a surface temperature of from 170° F to 200° F when flying in clear air. Immediately upon entering a cloud, the temperature drops very rapidly, sometimes by as much as 50° F in 1 second. Similarly, a rapid rise of temperature is observed on leaving a cloud. Small areas of clear air within a cloud and variations of cloud density are indicated by irregularities in the temperature trace. Figure 6 is an example of the response of this instrument during passage through various types of clouds. As indicated in the figure, the instrument is more sensitive to liquid-water drops than to snow. Thus, it is possible to identify regions containing liquid water in a continuous snow cloud.

MAXIMUM-DROP-SIZE CYLINDER

This device, which is described in reference 2, permits the determination of the angular extent of ice collected on a stationary cylinder 5 inches in diameter. With this information, the diameter of the largest drops present in significant quantity can be calculated. The angle is measured by visual observation of the edge of the ice formation against a scale consisting of white marks spaced at 10° intervals on the surface of the cylinder. When the values of maximum drop diameter from the stationary cylinder observations were compared with corresponding values of mean-effective diameter, as measured by the rotating cylinders, it was noted that in more than half the cases the indicated maximum diameter was less than the mean-effective diameter. This discrepancy was attributed mainly to the inability of the observer to identify the extreme edge of the ice formation. This error was always in the direction of a reduced observed angle, since it was the result of inability to detect thin ice accretions extending aft of the estimated point of termination. Another contributing factor is believed to be the effect on the water-drop impingement pattern of the slight change in cylinder profile due to the presence of the ice layer. To take account of these factors, it was decided to add a uniform correction of 5° to the observed position of the edge of the ice accretion. This correction was used in the calculation of all values of maximum diameter reported herein. Even with this correction, a considerable number of discrepancies of a scatter nature still remain. These can readily be explained by the effect of observational errors in both the cylinder methods. Although an attempt was made to read the angle between the stagnation point and the edge of the ice formation to the nearest 5°, it was found that three-fourths of the values recorded were multiples of 10°. This fact implies an uncertainty of approximately 5° in the estimated location of the edge of the ice accretion. The effect on the resulting values of maximum drop diameter of a 5° error in the location of the edge of the ice accretion is shown as curve A in figure 7. In addition to errors in maximum diameter, the errors in mean-effective diameter, as measured by the rotating cylinders, should also be considered. The maximum effect on calculated values of mean-effective diameter resulting from errors of up to 5 percent in the determination of the relative catch of the four cylinders over the range of rotating-cylinder diameters used in this investigation is shown as curve B in figure 7. These two sources of error are sufficient to account for the scatter in the observed data.

THE ROTATING-DISK ICING-RATE METER

The rotating-disk icing-rate meter used by the Ames Aeronautical Laboratory is a modification of the instrument developed by the Massachusetts Institute of Technology. (See references 8 and 9.) The rotating disk, measuring arm, and scraper are essentially the same as in the M.I.T. instrument. However, the magnetic method of measuring the thickness of ice on the edge of the disk has been replaced by a mechanical and optical system. In the Ames instrument, the movement of the measuring arm actuates a mirror which causes the image of a lamp filament to move along a slit. A moving photographic film which passes beneath the slit provides a continuous record of the position of the measuring arm.

Theory of the Instrument

This instrument has the following characteristics: (1) The displacement of the trace on the film, measured from the zero position, is directly proportional to the thickness of ice on the edge of the disk at the point of contact of the measuring arm; (2) the linear velocity of the film is directly proportional to the angular velocity of rotation of the disk; (3) a timing mechanism is provided to record equal time intervals on the film.

The methods used to determine liquid-water content, icing rate, and total ice collected during a period are derived in the following paragraphs:

The following symbols are used in the derivations:

A area on film between trace and zero position, square inches b diameter of disk, inches

E collection efficiency at a particular point on edge of disk

$\bar{E}$ over-all collection efficiency of disk or cylinder

E_{max} collection efficiency at front center point of disk

I icing rate on object having same over-all collection efficiency as disk, inches per hour

k instrument magnification ratio (y/σ)

n speed of rotation of disk, rpm

Q total ice accumulation on object having same over-all collection efficiency as disk, inches

s film advance per disk revolution, inches per revolution

t time, minutes

U local air velocity just forward of the rotating disk location, miles per hour

U^1 local air velocity just forward of the rotating-cylinder location, miles per hour

w liquid-water content (g/m^3)

x film travel, inches

y displacement of trace on film record from zero position, inches

z thickness of edge of disk, inches

Δ increment

ρ density of ice on disk, grams per cubic centimeter

σ thickness of ice on edge of disk at measuring point, inches

The rate of ice accumulation on the edge of the disk is given by

$$0.0173\ \bar{E}wUzb \quad \text{grams per minute}$$

and also by

$$0.273 \; Izb\rho \quad \text{grams per minute}$$

The rate at which ice passes under the measuring arm is given by

$$16.39 \; \sigma z \rho \pi b n \quad \text{grams per minute}$$

The numerical factors in the preceding expressions are determined by the units used.

When the icing rate is uniform, the ice passes under the measuring arm at the same rate as it is accumulated on the forward edge of the disk.[5] Thus, the following equations may be written:

$$16.39 \; \sigma z \rho \pi b n = 0.0173 \; \bar{\bar{E}} w U z b \tag{1}$$

and

$$16.39 \; \sigma z \rho \pi b n = 0.273 \; Izb\rho \tag{2}$$

equation (1) reduces to

$$\sigma = 1.056 \times 10^{-3} \frac{\bar{\bar{E}} U w}{\pi n \rho} \quad \text{inches}$$

The thickness of ice σ is related to the rate of generation of area under the recorder trace as follows:

$$\Delta A = y \Delta x = y s n \Delta t = k \sigma s n \Delta t \tag{3}$$

hence

$$\frac{\Delta A}{\Delta t} = k \sigma s n = \frac{1.056 \times 10^{-3} \; U \bar{\bar{E}} w k s}{\pi \rho} \tag{4}$$

The liquid-water content is therefore given by

$$w = \frac{10^3 \pi}{1.056 \; ks} \frac{\Delta A}{\Delta t} \frac{1}{U} \frac{\rho}{\bar{\bar{E}}}$$

[5]The response of the instrument to nonuniform icing conditions is discussed hereinafter.

For the Ames Laboratory instrument, $k = 36$ and $s = 2.183$, hence

$$w = 37.9 \frac{\Delta A}{\Delta t} \frac{1}{U} \frac{\rho}{\bar{E}} \tag{5}$$

The icing rate in inches per hour on a fixed object having the same average collection efficiency as the disk is obtained from equations (2) and (3) as follows:

$$I = 60n\pi\sigma = \frac{60\pi}{ks} \frac{\Delta A}{\Delta t}$$

$$I = 2.40 \frac{\Delta A}{\Delta t} = 2.40\ y \frac{\Delta x}{\Delta t} \tag{6}$$

The total ice accumulated over a period of time on such an object is

$$Q = \frac{\Sigma I \Delta t}{60} \doteq 0.04\ A \tag{7}$$

When the instrument was designed it was intended to use y rather than $\frac{\Delta A}{\Delta t}$ as a measure of the icing rate. However, unexpected gradual variations in the speed of the driving motor made it necessary to use areas. Moreover, the area method is more convenient when it is desired to calculate the total ice accumulation or the average over an interval. Values of maximum icing rate or icing rate at a particular time can be obtained from measurements of y, since

$$\frac{dA}{dt} = y \frac{dx}{dt}$$

Since this method of using the data does not require a constant speed of rotation of the disk, the range and sensitivity of the instrument can be improved considerably by using a variable-speed driving motor and adjusting the speed for variations in the severity of the icing conditions.

Empirical Calibration of the Instrument

It is seen from equation (5) that, in addition to the local air velocity U, the quantity $\rho/\bar{E}$ must be known in order to obtain w from the icing-rate-meter data. Values of this factor were obtained from simultaneous flight measurements with the multicylinder apparatus and the rotating-disk instrument. In the calculation of w from rotating-cylinder data, the quantity $U^1 w \bar{E} \Delta t$ is plotted as a function of cylinder radius and the curve is extrapolated to zero cylinder radius by means of data from reference 7. This yields values of $U^1 w \Delta t$, since the collection efficiency approaches unity as the radius approaches zero.

The exact time intervals during which the cylinders were exposed were located on the time scale of the rotating-disk record by means of a relay and the corresponding increments of area under the rotating-disk recorder trace were used with values of $U^1 w \Delta t$ from the rotating cylinders to calculate $\overline{E}/\rho$ by the following equation which follows from equation (5):

$$\frac{\overline{E}}{\rho} = \frac{37.9 \Delta A}{U^1 w \Delta t} \frac{U^1}{U}$$

The quantity $\frac{U^1}{U}$, which depends upon the location of the instruments with respect to the airplane, was determined as a function of the indicated airspeed by means of static pressure measurements at both locations.

Values of $\overline{E}/\rho$ determined in this way, plotted as a function of mean-effective drop diameter are presented in figure 8. Average values of $\overline{E}/\rho$ for various drop-size intervals and an approximate regression line determined by these group averages are also included in the figure. The standard deviation of the observed values of $\overline{E}/\rho$ from the regression line is 0.21, and the standard deviation from the average (1.11) is 0.24. This gives an indication of the reliability of the values of liquid-water content derived from the rotating-disk data. Since the standard deviation from the average value of $\overline{E}/\rho$ is only slightly greater than that from the regression line, the average value, $\overline{E}/\rho = 1.11$, was used in calculating the values of liquid-water content presented herein. In cases where the drop size is known, more accurate values of liquid-water content may be obtained by using the regression line.

Lag and Averaging Properties of Disk

Since the thickness of ice collected at a point during its passage across the front of the disk is measured after it has moved around to the rear side, there is a certain time lag in the response of the instrument, and the indicated icing rate is an average over a period rather than an instantaneous value. For this reason, the time scale used in recording and interpreting the icing-rate-meter data was set backward by an amount represented by the distance traveled by the film while a fixed point on the disk moves from the front stagnation point to the point of contact with the measuring arm. With this time scale, the indicated icing rate at a particular time, t, represents an average over a period from $t - \frac{1}{2}\Delta t$ to $t + \frac{1}{2}\Delta t$ where Δt is the time required for a point on the disk to move through the area of collection.

In order to determine the extent and distribution of the collection along the edge of the disk, several tests were made in which a quantity of ice was allowed to accumulate while the disk was stationary and then measured in a single revolution of the disk. The average of the results of five such tests is shown in figure 9 which gives the percent of the total ice which is contained within an angle of $\pm\theta$ measured from the midpoint of the collection area as a function of the angle, θ.

It is seen from the figure that the ice accretion extends through an angle of 74° on each side of the midpoint and that 95 percent of the ice is contained within 60° of the midpoint. On the basis of these results, the effective angle of collection is taken as 120°, which corresponds to a period of 10 seconds at 2 rpm; hence, the indicated icing rate at a particular time, t, is interpreted as an average over the period from $t - 5$ seconds to $t + 5$ seconds.

To illustrate the effect of the averaging process, the data of figure 9 were used to calculate the response of the instrument to uniform, sharp-edged clouds at 2 rpm. In figures 10(a), (b), and (c), the rectangles represent assumed uniform distributions of icing rate over periods of 7, 12, and 15 seconds, respectively, and the curves show the calculated response of the instrument. It is noted that for periods of uniform icing of less than 12 seconds duration, the maximum icing rate indicated by the instrument is less than the actual value; a 10-second period of icing would give a maximum of 95 percent of full response. It is also noted that, in terms of the time scale used herein, the response of the instrument begins 6 seconds before entering icing conditions and continues for 6 seconds after leaving.

In the construction of figure 10(d), the duration of flight through two small clouds was obtained from the record of the cloud indicator, and a uniform icing rate sufficient to make the maximum ordinate of the derived response curve equal to the observed maximum response of the instrument was chosen. The calculated response curve and the actual record of the instrument are shown for comparison. The close agreement between the two curves indicates that the variations in icing rate recorded by the icing-rate meter in this case were due primarily to the distribution of cloud masses in space rather than to variations in liquid-water content within a cloud.

The Collection Efficiency of the Rotating Disk

The data of figure 9 furnish a means of estimating the collection efficiency of the disk. Data from figure 9 have been used to prepare figure 11 which presents the ratio of the collection efficiency at any point on the edge of the disk to the collection efficiency at the stagnation point as a function of the sine of the angle from the stagnation point. In this figure, the area under the curve represents the ratio of the over-all collection efficiency to the efficiency at the stagnation point. Since the variation in relative collection efficiency is small near the midpoint, it is reasonable to assume that the maximum collection efficiency at the front of the disk is the same as that of a long ribbon of the same width, in this case 1/32 inch. It is shown in reference 9 that the collection efficiency of a 1/32-inch ribbon is practically 100 percent for all drops over 10 microns in diameter. Measurement of the area under the curve of figure 11 gives a value of 0.83 for the average collection efficiency of the entire disk during the five test runs used to construct the figure. Since the actual values of drop size for these five cases are unknown, a reasonable assumption is that the average value of $\overline{E}/\rho$ for these cases was the same as the average for all observations, 1.11. This gives a value of 0.75 g/cm^3 for the density of the ice. This value of ice density was used with values of $\overline{E}/\rho$ taken from the regression line of figure 10 to determine probable values of average collection efficiency of the disk for various values of drop size. The results are given in the following table:

Collection Efficiency of Icing-Rate Meter		
Drop diameter	$\overline{E}/\rho$	$\overline{E}$ (ρ = 0.75)
10	0.88	0.66
15	1.02	.76
20	1.13	.85
25	1.19	.89
30	1.22	.91
35	1.23	.92

Actual values of collection efficiency and ice density are not required in the determination of liquid-water content from the records of the icing-rate meter since the experimentally determined values of $\overline{E}/\rho$ are used in the calibration. These results are of interest, however, for comparison with the assumed values used in the preparation of the calibration charts included in reference 9. In that report, an over-all collection efficiency of 1.0 was assumed for all drops larger than 10 microns in diameter and 0.9 was used as a standard ice density. This gives a value of 1.11 for $\bar{E}/\rho$ which is exactly the same as that determined experimentally in this investigation; hence the two calibration procedures lead to the same values of liquid-water content.

REFERENCES

1. Lewis, William: A Flight Investigation of the Meteorological Conditions Conducive to the Formation of Ice on Airplanes. NACA TN 1393, 1947.

2. Lewis, William, Kline, Dwight B., and Steinmetz, Charles P.: A Further Investigation of the Meteorological Conditions Conducive to Aircraft Icing. NACA TN 1424, 1947.

3. Jones, Alun R., and Lewis, William: Recommended Values of Meteorological Factors to be Considered in the Design of Aircraft Ice-Prevention Equipment. NACA TN 1855, 1945.

4. Jones, Alun R.: An Investigation of a Thermal Ice-Prevention System for a Twin-Engine Transport Airplane. NACA Rep. 862, 1946.

5. Gumbel, E. J.: On the Frequency of Extreme Values in Meteorological Data. Bulletin of the American Meteorological Society. Vol. 23, Mar. 1942, pp. 95-105.

6. Peppler, Wilhelm: Unterkuhlte Wasserwolken und Eiswolken. (Supercooled water and ice clouds.) Forschungsund Erfahrungsberichte des Reichswetterdienstes, Ser. B, No. 1, Berlin, 1940. (Brief Summary in Bulletin of the American Meteorological Society. Vol. 29, Nov. 1948, p. 458.)

7. Langmuir, Irving, and Blodgett, K. B.: A Mathematical Investigation of Water Droplet Trajectories. General Electric Research Laboratory, July 1945.

8. Vonnegut, B., Cunningham, R. M., and Katz, R. E.: Instruments for Measuring Atmospheric Factors Related to Ice Formation on Airplanes. Mass. Inst. of Tech., Dept. of Meteorology, De-Icing Research Lab., Apr. 1946.

9. Katz, R. E., and Cunningham, R. M.: Aircraft Icing Instruments. Instruments for Measuring Atmospheric Factors Related to Ice Formation on Airplanes. – II. Mass. Inst. of Tech., Dept. of Meteorology, De-Icing Research Lab., Mar. 1948.

TABLE I.– METEOROLOGICAL DATA OBTAINED DURING OPERATIONS IN ICING CONDITIONS IN 1948

Flt. No.	Date	Time (MST)	Duration of rotating cylinder exposure (sec)	Average true air-speed (mph)	Pressure altitude (ft)	Free-air temperature (°F)	Liquid-water content [a] w_1 (g/m³)	Liquid-water content [a] w_2 (g/m³)	Mean-effective drop diameter (microns)	Drop-size distribution [b]	Maximum drop diameter (microns)	Cloud type [c]	State of cloud particles [d]	Air-mass classification [e]	Location and remarks
151	2-4-48	1647	160	179	13,500	-7	0.07	---	47	E	20	Cu	L	mPk	Central California; west slope of Sierra Nevada Mountains. Post-cold-frontal cumulus clouds.
		1700	155	170	7,400	17	.33	---	22	E	18	Cu	L		
		1705	230	148	5,900	21	.23	---	17	A	14	Cu	L		
		1725	69	151	8,900	10	.41	---	32	B	23	Cu	L		
		1729	35	154	10,400	4	.24	---	26	E	24	Cu	L		
152	2-6-48	1514	105	167	11,200	1	.36	---	18	A	32	Cu	L	mPk	Central California; Sierra Nevada and coastal mountains. Post-cold-frontal cumulus clouds.
		1546	165	175	7,000	17	.41	---	18	E	20	Cu	L		
		1550	165	159	7,100	17	.23	---	19	–	19	Cu	L		
		1553	80	153	7,000	17	.40	---	20	E	26	Cu	L		
		1607	58	144	8,200	13	.97	---	22	E	28	Cu	L		
		1613	140	139	9,300	8	.63	---	27	A	22	Cu	L		
153	2-7-48	1631	170	192	6,900	21	.11	---	50+	E	18	Ac	L	mP	Western Washington.
		1638	180	176	6,900	20	.05	---	50+	E	26	Ac	L	mP	Prefrontal convergence zone.
154	2-8-48	1415	180	171	9,300	10	.10	---	22	A	25	As-Ac	ML	mP	Western Washington. Complex cyclonic cloud formation with widespread precipitation.
		1419	180	183	9,300	10	.02	---	23	–	22	As-Ac	MS		
		1455	180	194	12,300	-2	.04	---	8	E	9	As-Ac	MS		
		1518	180	190	7,000	15	.004	---	50+	E	19	Cb	MS		
		1535	173	168	7,000	15	.01	---	12	E	15	Cb	MS		
		1556	30	173	8,300	7	.52	---	25	E	50+	Cb	ML		
		1617	78	158	4,700	21	.38	---	23	E	18	Cu	L		
155	2-9-48	1501	210	162	9,600	2	.56	---	29	A	23	Cb	ML	mPk	Western Washington. Unstable showery conditions in cyclonic onshore flow. Lightning flash observed at 1541 MST.
		1513	80	168	10,400	-1	.21	---	27	A	19	Cb	ML		
		1516	82	154	9,300	3	.44	---	26	A	23	Cb	ML		
		1519	116	152	9,500	2	.42	---	24	A	23	Cb	ML		
		1541	177	160	8,000	9	.55	---	18	C	17	Cu	L		
		1546	35	155	8,700	6	.23	---	18	A	18	Cb	ML		
		1550	84	155	8,700	6	.22	---	18	C	18	Cb	ML		
		1554	52	149	8,500	6	.10	---	15	A	18	Cu	L		
		1557	104	150	8,100	8	.52	---	18	A	18	Cu	L		
		1601	33	157	8,100	9	.54	---	15	A	15	Cb	ML		
		1635	33	170	7,800	10	.37	---	22	E	22	Cu	L		
		1641	27	141	5,700	18	.67	---	14	E	18	Cu	L		
		1650	21	167	6,300	16	.55	---	21	E	20	Cb	ML		
		1723	45	149	7,700	10	.55	---	13	D	20	Cu	L		
		1726	40	156	7,500	10	.39	---	16	A	18	Cu	L		
		1729	45	132	7,300	11	.82	---	15	A	18	Cu	L		
156	2-10-48	1730	211	188	13,000	-15	.02	---	8	A	13	Ac	L	mP	Southeastern Idaho. Cold low over Colorado and Wyoming.
		1734	180	195	13,000	-15	.03	---	12	A	15	Ac	L		
159	2-13-48	1159	90	156	2,000	27	.08	---	20	E	50+	Fs	R&L	mT/cP	Indianapolis to St. Louis. Freezing rain associated with low over southern Indiana.
		1204	180	154	2,000	26	.09	---	18	E	50+	Fs	R&L		
		1232	155	136	1,300	25	.01	---	50+	–	50+	Ns	R&MS		
		1239	180	150	2,500	20	.04	---	9	A	14	St	L		
166	3-8-48	1755	30	160	12,400	11	.35	.47	33	A	44	Cu	L	mPk	Central California; west slope of Sierra Nevada Mountains. Directly behind cold front.
		1800	110	166	11,600	11	.18	.31	50+	E	44	Cu	L		
		1807	56	162	10,800	14	.03	.14	19	A	–	Cu	L		
		1811	50	150	11,400	12	.32	.47	56	E	45	Cb	ML		
		1814	35	183	11,200	14	.23	.54	44	E	42	Cb	ML		
		1816	38	181	11,200	12	.14	.20	--	–	43	Cu	L		
167	3-9-48	1407	80	206	14,600	-3	.24	.31	19	D	19	Cu	L	mPk	Southern Nevada, northern Arizona, and northwestern New Mexico. Cyclonic conditions with low center over southwestern Utah. North-south lines of cumulonimbus clouds along mountain ranges. Diffuse front encountered at about 1600 MST.
		1410	55	189	14,200	-2	.23	.26	19	D	23	Cu	L		
		1413	64	174	14,500	-4	.18	.29	21	A	–	Cb	ML		
		1416	27	188	14,400	-4	.08	.22	9	E	–	Cu	L		
		1419	134	169	14,700	-5	.10	.20	22	A	21	Cb	MS		
		1423	88	180	15,100	-6	.05	.42	18	A	20	Cu	L		
		1430	56	174	15,200	-6	.11	.28	24	A	20	Cb	ML		
		1455	75	176	14,700	-4	.05	.38	17	A	20	Cb	MS		
		1502	67	175	15,700	-6	.04	.27	27	E	20	Cb	MS		
		1509	62	164	14,400	-2	.17	.39	20	A	21	Cu	L		
		1522	93	164	14,700	-4	.01	.12	28	E	21	Cb	MS		
		1602	330	205	16,200	-5	.01	.13	18	A	14	Cb	MS		
		1625	76	188	18,700	-14	.17	.35	22	A	19	Cb	ML		
		1649	134	176	14,500	5	.28	.36	20	A	14	Cb	ML		
		1700	28	183	13,400	9	.38	.59	17	A	15	Cu	L		
170	3-12-48	1330	130	168	10,000	15	.02	.09	18	A	17	Ac-As	MS	mP	Southwestern Washington, western Oregon, and offshore along Oregon coast. Stratiform clouds in area of convergence south of low center.
		1333	176	161	10,100	15	.03	.22	33	A	30	Ac-As	MS		
		1345	225	190	10,000	15	.11	.13	14	A	43	Ac-As	ML		
		1353	100	179	10,200	14	.07	.15	14	A	16	Ac-As	ML		
		1356	199	175	10,300	13	.12	.18	16	A	16	Ac-As	ML		
		1406	240	183	10,200	14	.12	.15	23	C	16	Ac-As	ML		
		1420	270	184	9,900	13	.08	.09	10	A	43	Ac-As	ML		
		1426	180	188	10,100	14	.06	.10	15	A	43	Ac-As	L		
		1434	159	180	10,150	14	.03	.13	16	A	34	Ac-As	ML		
		1445	120	169	6,800	24	.34	.34	18	A	17	Sc	ML		
		1449	29	163	6,500	26	.06	.10	12	A	21	Sc	L		
		1452	66	164	6,900	24	.22	.36	11	E	17	Sc	ML		
		1457	81	164	6,400	24	.32	.34	15	A	15	Sc	L		
		1551	36	189	8,700	16	.03	.11	20	A	–	Sc	ML		
		1553	70	190	8,300	16	.19	.22	24	C	29	Sc	L		
		1602	210	194	8,000	18	.01	.04	15	A	29	Sc	ML		

[a] w_1 represents the average liquid-water content during the entire period of exposure of the rotating cylinder. w_2 represents the average liquid-water content during that part of the exposure period during which the actual presence of cloud drops was indicated by the cloud indicator. Values of w_2 were not obtained prior to flight 166 as the cloud-indicator and rotating-cylinder records were not accurately synchronized.

[b] Drop-size distributions as indicated by the rotating-cylinder data are given according to the scale defined in reference 7. These results are regarded as unreliable.

[c] Cloud types are given according to the International Classification: Cu, cumulus; Cb, cumulonimbus; St, stratus; Sc, stratocumulus; Fs, fractostratus; Ns, nimbostratus; Ac, altocumulus; As, altostratus; Ac-As, altocumulus associated with altostratus; Acc, altocumulus castellatus.

[d] L, liquid cloud drops; S, snow crystals; ML, mixed snow crystals and liquid cloud drops, liquid predominant; MS, mixed snow crystals and liquid cloud drops, snow predominant; R, rain.

[e] m, Maritime; c, continental; P, polar; T, tropical; k, tending to become unstable in the lower layers.

NACA

Flt. No.	Date	Time (MST)	Duration of rotating cylinder exposure (sec)	Average true air-speed (mph)	Pressure altitude (ft)	Free air temperature (°F)	Liquid-water content[a] w_1 (g/m³)	Liquid-water content[a] w_2 (g/m³)	Mean-Effective drop diameter (microns)	Drop-size[b] distribution	Maximum drop diameter (microns)	Cloud type[c]	State of cloud particles[d]	Air-mass classification[e]	Location and remarks
171	3-13-48	1320	16	196	8,700	16	.18	.21	11	A	22	Cu	L	mPk	Southwestern Oregon and northwestern California over coastal mountains. Scattered to broken cumiliform clouds usually with precipitation in low-pressure trough along coast.
		1322	155	199	9,400	16	.36	.39	10	E	28	Cu	L		
		1325	51	153	8,400	14	.36	.38	29	C	30	Cb	ML		
		1329	151	162	9,550	11	.56	.65	27	A	26	Cb	ML		
		1341	98	169	8,900	11	.23	.36	26	E	41	Cb	ML		
		1347	70	147	8,550	11	.08	.36	21	A	20	Cu	L		
		1355	146	165	8,100	16	.35	.59	23	E	19	Cb	ML		
		1402	33	185	8,200	15	.34	.36	21	E	22	Cb	ML		
		1405	21	171	8,300	15	.14	.21	11	D	22	Cu	L		
		1408	58	186	8,500	15	.33	.48	45	A	29	Cb	ML		
		1419	76	169	8,200	18	.31	.48	21	A	19	Cb	ML		
		1425	79	165	7,800	17	.45	.59	21	E	22	Cu	L		
		1430	224	158	9,200	13	.13	.25	19	A	19	Cb	ML		
		1506	163	171	7,700	16	.22	.50	18	A	22	Cu	L		
		1531	268	157	12,000	3	.44	.56	35	A	30	Cb	ML		
		1607	99	190	11,800	2	.79	.88	20	E	28	Cu	L		
		1615	125	192	11,800	2	.18	.72	21	A	28	Cb	ML		
174	3-19-48	1402	180	179	11,400	2	.83	.88	12	A	11	Cu	L	mPk	Central California near Mt. Diablo. Heavy cumuli without precipitation about 15 hours after cold front passage.
		1408	69	140	11,500	2	1.08	1.15	11	A	17	Cu	L		
		1415	94	171	12,200	–2	.70	.92	9	A	11	Cu	L		
175	3-22-48	1232	240	197	13,000	18	.07	.14	23	A	19	As–Ac	MS	mPk	San Francisco to Seattle along coast and over coastal mountains. Traversed frontal altostratus from 1230 to 1330 with negligible icing. Encountered icing in post-cold-front cumiliform clouds in Oregon and Washington.
		1358	118	171	7,900	18	.03	.07	24	A	19	As–Ac	MS		
		1409	89	163	6,700	20	.05	.17	45	A	47	Cb	MS		
		1414	77	172	7,300	17	.15	.27	24	A	37	Cu	L		
		1419	60	175	6,000	18	.08	.28	20	E	25	Cu	L		
		1423	110	160	6,700	17	.11	.23	25	A	37	Cb	ML		
		1439	210	189	8,800	11	.16	.24	25	A	34	Cb	ML		
		1455	58	178	8,000	13	.48	.69	20	B	22	Cu	L		
		1505	158	164	8,900	11	.44	.56	20	A	23	Cb	ML		
		1511	72	172	9,200	9	.63	.68	22	A	22	Cb	ML		
		1514	120	151	9,700	8	.15	.26	23	C	23	Cb	ML		
		1519	100	179	9,900	6	.42	.95	32	A	29	Cb	ML		
		1527	278	170	9,800	4	.21	.46	26	A	22	Cb	MS		
		1534	84	177	10,300	2	.59	.63	31	A	29	Cb	ML		
176	3-23-48	1402	120	181	9,900	13	.22	.37	13	A	18	Cu	L	mPk	Near Medford, Oregon. Cyclonic flow in low-pressure trough.
		1408	230	186	8,800	15	.18	.29	16	A	16	Cu	L		
		1415	186	167	11,500	10	.41	.54	25	A	21	Cu	L		
		1421	71	154	11,900	11	.42	.53	27	C	25	Cu	L		
		1624	191	164	11,600	13	.12	.33	27	A	29	Cb	ML		
		1655	117	158	10,200	14	.31	.68	28	A	23	Cb	ML		
		1703	119	163	9,800	18	.26	.37	26	A	23	Cb	ML		
177	3-24-48	1329	186	166	13,000	–3	.01	.10	50+	–	50+	Cb	MS	mPk	Northern California, 10 to 15 miles offshore. Cyclonic flow in low-pressure trough.
		1451	30	173	8,800	15	.15	.28	26	–	45	Cu	L		
		1458	43	176	9,100	17	.30	.58	27	A	45	Cb	ML		
		1505	30	182	9,300	16	.29	.43	29	A	43	Cb	ML		
179	3-29-48	1203	45	197	13,700	7	.69	.78	23	A	27	Cb	ML	mP	Central California, west slope of Sierra Nevada and coastal mountains. Weak high-pressure ridge. Convective clouds in moist air mass with wet-adiabatic lapse rate.
		1217	41	215	13,700	6	.14	.26	28	A	26	Cu	L		
		1225	174	202	11,800	13	.20	.74	23	A	23	Cb	ML		
		1232	71	185	11,700	14	.53	.64	23	A	24	Cb	ML		
		1239	91	174	12,100	13	.66	.98	24	A	15	Cu	L		
		1244	72	167	11,750	12	.39	.61	18	C	17	Cb	ML		
		1248	46	178	11,500	13	.41	.61	32	D	20	Cb	ML		
		1257	132	154	11,400	14	.83	.98	25	E	22	Cu	L		
		1302	96	174	10,400	16	.68	.88	23	E	22	Cu	L		
		1315	30	173	11,600	13	.76	.84	20	E	22	Cu	L		
		1329	10	169	13,600	5	.28	.40	–	–	–	Cb	ML		
		1333	19	206	14,800	5	.29	.46	23	A	26	Cb	ML		
		1353	161	179	15,700	4	.09	.14	26	A	27	Cb	MS		
		1400	77	187	14,500	6	1.63	1.72	24	E	19	Cb	ML		
		1426	27	189	14,600	6	.89	1.20	19	E	15	Cb	ML		
		1428	22	197	13,700	10	.64	.94	25	E	20	Cu	L		
		1547	106	180	11,800	15	1.10	1.10	25	E	28	Cu	L		
180	3-30-48	1311	214	175	16,200	1	.05	.06	12	A	16	Ac	L	mP	Near Lake Tahoe. Single lenticular cloud over Sierra summit.
		1318	117	159	15,900	0	.03	.03	8	A	–	Ac	L		
		1323	121	188	16,200	–1	.03	.04	10	A	–	Ac	L		
181	4-2-48	1510	190	189	13,100	10	.18	–	22	E	28	Ac	L	mP	South of Mt. Shasta, Calif. Brief interval of light icing in extensive prefrontal precipitation area.
		1515	270	165	13,100	11	.008	.04	27	C	11	Ac–As	MS		
183	4-5-48	1405	60	188	12,700	–7	.42	.49	29	E	28	Cb	ML	mP	Northwest of Seattle. Complex cloud system in southwesterly flow ahead of low-pressure area.
		1426	100	246	11,450	2	.004	.04	15	A	24	Ac–As	MS		
		1431	107	180	10,900	3	.25	.37	21	C	21	Cu	L		
		1436	35	193	11,600	–3	.83	1.16	20	A	20	Cu	L		
		1449	192	165	14,700	–12	.003	.04	10	A	–	Ac–As	MS		
		1514	91	185	14,650	–13	.02	.03	20	E	10	Ac	ML		
		1521	86	211	9,500	6	.17	.19	46	E	12	Ac	ML		
		1527	219	158	9,200	10	.05	.09	31	E	23	Ac–As	MS		
		1533	55	189	9,000	9	.15	.18	50+	E	–	Ac	ML		
		1545	204	137	9,400	6	.04	.08	27	A	28	Ac–As	ML		
		1554	116	178	8,000	14	.04	.09	24	A	–	Ac–As	ML		
		1559	201	197	7,900	12	.23	.28	37	E	–	Ac	ML		
		1610	199	173	7,900	12	.18	.24	47	E	39	Ac	ML		
		1618	234	177	8,000	12	.06	.10	17	A	22	Ac	L		
		1629	271	179	8,000	14	.15	.19	23	A	13	Ac	ML		
		1635	128	172	8,000	10	.19	.28	18	A	17	Ac	ML		
		1641	310	176	8,100	10	.13	.17	21	A	22	Ac	ML		
		1726	288	183	8,100	13	.10	.13	21	A	21	Ac	ML		

See footnotes a, b, c, d, and e, p. 26

NACA

Flt. No.	Date	Time (MST)	Duration of rotating cylinder exposure (sec)	Average true airspeed (mph)	Pressure altitude (ft)	Free-air temperature (°F)	Liquid-water content[a] w_1 (g/m³)	Liquid-water content[a] w_2 (g/m³)	Mean-effective drop diameter (microns)	Drop size[b] distribution	Maximum drop diameter (microns)	Cloud type[c]	State of cloud particles[d]	Air-mass classification[e]	Location and remarks
184	4-6-48	1326	129	214	17,800	-22	.02	.06	19	B	22	Ac	ML	mPk	Central Washington. West to southwest flow with upper low offshore.
		1331	52	205	17,000	-22	.11	.21	25	E	26	Cb	ML		
		1345	109	199	16,900	-23	.07	.15	18	A	–	Cb	ML		
185	4-6-48	1755	151	202	15,700	-19	.13	.25	24	E	12	Cb	ML	mPk	Central Oregon and northeastern California.
		1818	64	221	16,700	-20	.18	.26	42	E	26	Cb	ML		
		2010	58	202	8,900	14	.48	.61	22	E	25	Cu	L		
186	4-9-48	1251	76	192	12,000	12	.03	.08	14	A	26	Ac	L	mPk	Northern California and southwestern Oregon. Cyclonic flow with low center west of Portland.
		1259	78	181	10,900	14	.04	.06	23	A	31	Ac	L		
		1310	90	167	10,600	16	.28	.32	39	D	–	Ac	L		
		1340	108	184	11,200	13	.12	.16	37	E	29	Ac	L		
		1353	182	165	12,400	9	.14	.15	29	E	27	Ac	ML		
187	4-10-48	1234	146	205	8,900	14	.15	.24	20	C	20	Sc	L	mP	Southern Oregon, northern Nevada, northern Utah, and southern Wyoming. Post-cold-frontal conditions with low over Colorado.
		1441	57	206	12,700	6	.38	.45	16	C	16	Cu	L		
		1524	176	204	13,300	5	.08	.17	17	A	14	Ac	L		
		1540	211	190	13,100	8	.03	.08	13	A	–	Ac-As	MS		
		1559	205	203	13,000	12	.28	.39	22	B	30	Cu	L		
		1605	144	194	12,900	12	.12	.24	21	B	22	Cu	L		
		1624	192	193	13,200	12	.05	.12	10	A	50	Ac	ML		
189	4-12-48	1334	45	149	8,000	22	.55	.65	22	D	–	Cu	L	mPk and cP	Western Nebraska. Small low with weak cold front in western portion.
		1346	149	193	7,900	20	.03	.20	18	A	–	Cu	L		
		1405	296	164	8,400	21	.07	.26	12	A	11	Cu	L		
		1412	124	208	9,000	20	.03	.23	11	A	–	Cu	L		
		1436	227	187	10,900	12	.06	.09	17	A	16	Ac	ML		
		1443	218	186	11,100	11	.11	.14	20	B	16	Ac	L		
		1450	166	173	11,100	11	.10	.16	20	B	21	Ac	ML		
		1459	366	185	11,400	9	.03	.08	15	A	16	Ac	ML		
		1508	121	182	7,800	17	.22	.69	26	E	22	Cb	ML		
193	4-16-48	1122	159	170	10,000	25	.08	.31	11	A	–	Ac	L	cP	Michigan. Altocumulus along cold front near Detroit. Stratocumulus in cold air mass following front.
		1130	145	168	9,900	25	.06	.30	6	A	9	Ac	L		
		1142	280	194	11,100	16	.08	.25	10	A	12	Ac	L		
		1222	298	164	5,800	25	.20	.28	13	B	17	Sc	L		
		1253	157	164	4,300	23	.27	.29	14	B	14	Sc	L		
		1258.	171	169	4,200	19	.10	.13	12	A	14	Sc	L		
194	4-17-48	1249	92	185	13,100	23	.003	.03	7	A	–	Acc	L	cTk/cP	Central Iowa. Area of falling pressure ahead of warm front.
		1255	267	164	14,600	21	.07	.24	13	A	13	Acc	L		
		1301	350	182	15,400	13	.03	.18	15	A	16	Acc	ML		
		1318	188	173	15,700	13	.15	.20	14	C	16	Acc	ML		
195	4-18-48	1402	188	189	20,200	-8	.04	.12	11	A	11	Cb	ML	cTk	Southeastern Wyoming and northeastern Colorado. Low centered over Nebraska extending to Colorado. Clouds formed in warm air ahead of slowly moving cold front.
		1411	91	212	21,100	-12	.24	.31	9	A	14	Cb	ML		
		1416	431	216	20,900	-9	.01	.09	10	A	16	Cb	MS		
		1426	123	162	21,900	-16	.08	.23	12	A	14	Cb	ML		
		1432	241	191	23,000	-22	.13	.23	14	A	14	Cb	ML		
		1445	181	204	22,500	-19	.13	.25	13	A	14	Cb	ML		
		1450	339	204	23,000	-22	.12	.29	12	A	16	Cb	ML		
196	4-19-48	0929	358	128	13,400	11	.07	.18	15	A	17	Ac	L	cP	Southern Wyoming. Post-cold-frontal conditions with northwesterly flow. Low over Iowa.
		0943	353	213	13,900	5	.05	.09	15	A	13	Ac	MS		
		0951	171	180	13,700	6	.29	.29	23	A	23	Ac	ML		
		1003	84	196	13,700	5	.25	.33	21	A	27	Ac	L		
		1012	145	198	13,700	6	.17	.18	21	A	23	Ac	ML		
		1016	202	171	12,900	12	.26	.29	25	A	24	Ac	ML		
		1025	61	181	12,600	13	.04	.12	14	A	18	Ac	L		
197	4-30-48	1235	120	159	6,700	24	.05	.10	20	A	48	Cb	ML	mP	Offshore over Monterey Bay. Dissipating low about 300 miles north along coast.
198	5-4-48	1120	120	186	10,400	26	.04	.07	15	A	50+	Ac	L	mP	Northern California, western Oregon, and western Washington. Prefrontal cloud system in advance of low center 800 miles west of Seattle.
		1144	180	180	12,000	21	.07	.07	25	D	42	Ac	L		
		1156	151	175	12,100	20	.06	.07	50+	–	42	Ac	L		
		1330	64	185	6,800	22	.29	.37	17	E	35	Cu	L		
		1629	180	221	17,500	1	.05	.07	41	E	14	Ac	L		
		1634	210	209	17,400	3	.07	.07	19	E	14	Ac	L		
		1647	245	192	16,800	2	.08	.09	17	E	15	Ac	ML		
199	5-5-48	1324	183	210	17,700	-2	.003	.02	13	C	25	Ac-As	MS	mP	Northwest of Seattle. Prefrontal precipitation area. Low center off the coast of British Columbia.
		1350	118	212	11,800	21	.12	.16	36	E	38	Ac	L		
		1356	96	168	12,000	22	.28	.30	26	E	44	Ac	L		
		1430	93	193	18,600	-3	.06	.17	24	E	39	Ac-As	MS		
		1516	161	190	21,900	-12	.005	.01	–	–	–	Ac-As	MS		
		1545	78	224	19,200	-4	.02	.08	18	A	16	Ac-As	MS		
		1606	115	181	13,400	15	.15	.17	47	E	41	Ac-As	ML		
		1610	174	176	13,700	16	.08	.14	25	A	40	Ac-As	ML		
200	5-6-48	1353	35	183	11,000	14	.99	.99	23	A	24	Cu	L	mPk	Near Seattle. Post-cold-frontal conditions. Front in eastern Washington.
		1356	20	174	10,000	13	.82	1.36	21	E	25	Cu	L		
		1358	41	171	9,500	14	.56	.70	21	E	24	Cu	L		
		1403	41	183	9,100	14	.66	.69	24	E	25	Cu	L		
		1405	32	161	9,300	15	.59	.67	22	E	22	Cu	L		
		1412	11	191	10,500	9	.56	.68	23	E	21	Cu	L		
		1415	41	192	9,200	12	.63	.69	18	E	21	Cu	L		
		1417	66	180	9,000	14	.41	.45	19	E	25	Cu	L		
		1421	92	174	8,900	13	.06	.12	26	C	–	Cb	ML		
		1432	35	192	9,700	11	.48	.62	21	C	21	Cu	L		
		1435	46	178	9,200	13	.23	.39	22	A	22	Cb	ML		
		1437	54	189	8,900	14	.38	.50	22	A	29	Cu	L		
		1445	45	166	9,000	15	.54	.68	24	E	14	Cu	L		
		1450	75	187	8,500	14	.33	.49	21	E	22	Cu	L		
		1454	51	183	8,200	16	.53	.69	25	E	22	Cu	L		
		1514	171	192	11,100	6	.03	.08	22	B	16	Cb	MS		

See footnotes a, b, c, d, and e, p. 26

NACA

Flt. no.	Date	Time (MST)	Duration of rotating cylinder exposure (sec)	Average true airspeed (mph)	Pressure altitude (ft)	Free air temperature (°F)	Liquid-water content[a] w_1 (g/m³)	Liquid-water content[a] w_2 (g/m³)	Mean-effective drop diameter (microns)	Drop size distribution[b]	Maximum drop diameter (microns)	Cloud type[c]	State of cloud particles[d]	Air-mass classification[e]	Location and remarks
201	5-7-48	1404	48	171	13,300	0	.70	.88	21	B	18	Cb	ML	mPk	Seattle to Sacramento. Post-cold-frontal air mass. Front in Wyoming and Utah.
		1409	36	196	13,800	-5	.55	.86	24	A	23	Cb	ML		
		1428	59	184	15,500	-11	.07	.09	23	A	27	Cb	MS		
		1432	30	193	15,300	-10	.76	.95	24	A	26	Cb	ML		
		1437	64	174	15,000	-10	1.15	1.27	22	A	24	Cu	L		
		1445	64	161	14,600	-7	1.23	1.33	24	B	28	Cb	ML		
		1449	31	154	14,800	-6	.01	.03	26	A	21	Cb	MS		
		1512	32	214	14,400	-7	.01	.02	–	–	38	Cb	MS		
		1618	84	172	9,000	14	.006	.03	18	A	17	Ac-As	ML		
		1633	120	167	10,500	8	.04	.10	14	A	13	Ac-As	MS		
		1639	25	196	11,300	4	.22	.26	22	A	28	Ac-As	ML		
		1704	50	202	11,700	6	.29	.39	24	E	28	Cb	ML		
202	5-12-48	1445	137	193	19,700	-1	.06	.06	15	B	19	Ac	L	mP	Northern California and western Oregon. Entire flight in frontal zone. Observations mostly in warm air mass above occluded front. Last three observations in cold air behind front.
		1459	267	178	19,500	1	.06	.06	13	C	17	Ac	L		
		1507	234	160	20,000	-2	.02	.03	24	C	20	Ac	L		
		1526	338	178	19,900	-1	.10	.10	19	A	20	Ac	L		
		1534	240	198	19,600	0	.13	.14	19	A	19	Ac	L		
		1541	186	212	18,600	3	.11	.12	21	A	21	Ac	L		
		1549	170	189	19,000	4	.14	.14	17	A	36	Ac	L		
		1559	300	204	18,900	5	.10	.11	21	A	21	Ac	L		
		1606	250	202	18,800	5	.06	.07	16	A	22	Ac	L		
		1743	118	210	11,000	13	.14	.24	18	A	39	Ac	L		
		1746	82	200	10,000	16	.15	.22	22	A	42	Ac	L		
		1812	135	206	13,000	3	.06	.07	16	A	25	Ac	L		
203	5-13-48	1450	108	189	16,000	-16	.07	.14	22	A	40	Ac	L	mPk	Western Oregon. Weak high-pressure wedge. Cold front over Wyoming.
		1455	100	180	17,000	-17	.13	.18	24	A	26	Ac-As	ML		
		1522	141	208	16,800	-16	.09	.15	22	C	24	Ac-As	L		
		1600	123	181	16,000	-14	.16	.22	23	A	27	Ac-As	ML		
		1605	67	180	16,200	-14	.16	.19	21	A	27	Ac-As	ML		
		1617	161	182	15,900	-12	.04	.06	15	A	23	Ac-As	L		
		1626	201	173	16,200	-12	.04	.08	17	B	21	Ac-As	ML		
		1729	28	188	16,000	-8	.23	.43	26	B	26	Cb	ML		
204	5-14-48	1240	34	182	9,200	16	.08	.18	11	A	16	Cu	L	mPk	Western Idaho to eastern Montana. Post-cold-frontal conditions. Front across North Dakota and South Dakota.
		1243	29	184	9,200	17	.02	.06	–	–	16	Cu	L		
		1246	24	182	9,200	17	.04	.14	–	–	14	Cu	L		
		1257	91	177	11,000	9	.10	.17	17	A	16	Cu	L		
		1301	47	181	11,700	8	.19	.27	18	A	21	Cu	L		
		1304	45	193	11,400	8	.28	.41	19	A	24	Cu	L		
		1311	150	179	11,300	9	.16	.26	16	A	16	Sc	L		
		1317	193	163	12,200	6	.19	.29	18	A	22	Sc	ML		
		1327	183	173	13,200	4	.16	.21	18	B	24	Sc	ML		
		1332	92	189	13,000	7	.12	.21	19	A	20	Sc	ML		
		1506	51	197	16,500	-2	.09	.16	12	A	15	Cu	L		
		1514	89	199	15,800	-1	.06	.13	13	A	16	Ac	ML		
		1548	200	190	15,000	2	.18	.31	17	A	25	Cb	ML		
		1555	13	183	13,900	6	.16	.29	–	–	17	Cb	ML		
205	5-15-48	1105	170	178	8,900	22	.10	.12	12	D	13	Sc	L	cP	Western Minnesota to western New York. First part of flight was in post-cold-frontal conditions. Line of cumulonimbus clouds along cold front were encountered at 1330 near the west shore of Lake Michigan. Flight was conducted along and through frontal icing zone until 1413. Maximum width of icing zone was about 3 miles. Maximum duration of continuous icing in frontal zone was less than 2 minutes even when flying parallel to front.
		1113	36	158	9,800	20	.24	.45	9	B	15	Cu	L		
		1116	68	177	9,900	22	.16	.32	15	A	16	Sc	L		
		1119	125	174	9,900	20	.29	.34	15	A	16	Sc	L		
		1131	56	162	11,200	15	.23	.38	17	A	19	Cu	L		
		1135	114	183	11,200	15	.29	.46	17	B	18	Cu	L		
		1145	150	181	10,900	16	.13	.27	12	C	18	Ac	L		
		1214	37	198	11,800	14	.29	.45	12	D	17	Cu	L		
		1240	63	180	13,600	12	.44	.54	13	A	21	Cb	ML		
		1334	106	195	18,900	-3	.29	.55	25	B	49	Cb	ML		
		1358	94	188	16,000	7	.47	.63	24	B	27	Cb	ML		
		1402	177	173	16,000	7	.20	.44	18	D	22	Cb	ML		
		1408	180	182	16,200	7	.15	.37	21	A	27	Cb	ML		
		1430	119	210	17,500	5	.03	–	28	C	22	Ac-As	MS		
206	5-16-48	1233	240	203	21,200	-6	.004	.04	–	–	–	As	MS	mT	Near Cape May, N. J. Southern edge of precipitation area along occluded front.
		1333	39	242	14,100	17	.03	.07	15	C	20	Ac	L		
		1337	180	175	14,200	19	.13	.22	20	C	21	Ac	L		
		1345	140	180	14,500	18	.15	.21	20	C	21	Ac	L		
207	5-18-48	1227	184	191	16,600	-4	.14	.21	14	B	20	Ac-As	ML	cP	Pennsylvania and eastern Ohio. First part of flight in clouds associated with secondary cold front. Post-cold-frontal conditions after 1330 MST.
		1230	42	201	16,300	-2	.13	.18	13	A	–	Ac-As	ML		
		1232	162	168	16,600	-4	.05	.10	13	A	18	Ac-As	ML		
		1241	167	187	16,700	-4	.02	.05	11	C	17	Ac-As	ML		
		1321	155	197	13,900	7	.07	.12	8	A	15	Ac	L		
		1404	63	183	13,600	9	.94	1.16	19	E	16	Cu	L		
		1407	103	173	13,300	7	.54	.82	18	A	18	Cu	L		
		1411	104	154	13,800	9	.92	1.09	19	A	19	Cu	L		
		1420	47	193	13,600	7	.95	1.15	20	C	14	Cu	L		
		1422	56	177	13,600	8	.72	.78	17	A	18	Cb	ML		
		1424	54	170	13,800	8	.60	.79	15	A	21	Cb	ML		
		1429	25	193	13,900	8	1.10	1.71	8	E	15	Cu	L		
		1435	35	200	14,300	4	.85	1.24	14	A	15	Cu	L		
		1438	60	166	14,400	5	.71	1.00	13	A	16	Cu	L		
		1440	91	160	13,300	8	.82	1.04	18	A	17	Cu	L		
		1444	60	145	12,400	11	.47	.75	11	A	19	Cu	L		
		1513	40	173	12,200	17	.46	1.03	14	E	16	Cu	L		
209	5-20-48	1420	122	171	17,700	11	.17	.28	10	B	10	Ac	ML	mP	Southern Wyoming and central California. Weak low over Nevada and Utah. No fronts.
		1440	28	240	19,800	-1	.08	.16	9	D	10	Ac	L		
		1445	87	174	20,700	-6	.06	.12	10	A	12	Ac	ML		
		1811	70	210	12,100	10	.01	.04	10	D	36	Ac	L		
		1825	240	210	8,100	23	.04	.09	22	A	30	Sc	MS		
		1836	165	203	8,100	21	.19	.21	19	D	22	Sc	L		
		1840	148	202	8,200	21	.08	.10	15	A	16	Sc	L		

See footnotes a, b, c, d, and e, p. 26.

NACA

TABLE II.— LIQUID-WATER-CONTENT DATA OBTAINED WITH THE ROTATING-DISK ICING-RATE METER AVERAGED OVER VARIOUS ELAPSED TIME INTERVALS

Flight No.	Number of icing instances	Total time in measurable icing (min)	Total ice accumulation[b] (in.)	Average liquid-water content during measurable icing (g/m³)	Maximum duration of continuous icing (min)	Data for single icing instance giving greatest total ice accumulation: Total ice[b] (in.)	Duration (min)	Average liquid-water content (g/m³)	Maximum liquid-water content averaged over various elapsed time intervals (g/m³): 10 sec	1 min	5 min	20 min
151	17	13.7	0.58	0.22	3.0	0.17	1.5	0.48	0.98	0.64	0.30	0.081
152	16	29.8	2.66	.44	6.5	.78	6.5	.55	1.48	.77	.65	.381
153	5	7.6	.24	.14	2.6	.10	2.6	.14	.33	.21	.11	.051
154	14	11.7	.51	.20	3.0	.11	3.0	.17	1.16	.49	.16	.059
[a]155	31	32.1	2.59	.40	4.4	.27	2.2	.36	1.39	.75	.44	.158
[a]159	4	2.0	.05	.12	1.0	.02	1.0	.11	.43	--	--	---
166	16	20.8	.86	.19	2.9	.16	2.9	.26	.71	.49	.18	.126
[a]167	11	9.8	.36	.16	1.7	.09	1.7	.21	.54	.29	.21	.062
[a]170	22	41.5	1.05	.11	7.0	.23	4.4	.25	.52	.45	.28	.101
[a]171	35	34.5	2.32	.30	3.3	.37	3.3	.49	1.30	.67	.46	.157
174	12	13.5	1.68	.64	4.9	.86	4.9	.85	1.37	1.00	.83	.435
175	40	48.4	2.74	.26	4.4	.33	2.1	.75	1.09	.86	.54	.204
176	30	25.7	1.28	.23	2.2	.18	2.0	.43	.88	.62	.29	.131
177	7	4.5	.31	.31	.7	.10	.7	.73	1.09	.49	.11	.068
179	40	42.9	5.68	.60	4.6	1.03	4.2	1.07	2.00	1.82	1.01	.376
180	4	1.4	.04	.14	.9	.03	.9	.12	.20	.12	.03	.008
181	15	19.9	.42	.10	4.5	.19	4.3	.19	.36	.35	.17	.045
183	36	56.9	2.35	.18	6.4	.27	5.6	.24	1.37	.58	.22	.135
184	3	1.4	.14	.38	.8	.12	.8	.60	.99	.59	.12	.028
185	7	7.0	.58	.35	2.6	.32	2.6	.40	.77	.69	.30	.075
186	16	24.5	.80	.15	3.6	.16	3.6	.22	.53	.41	.17	.098
187	26	27.4	1.01	.16	4.3	.18	3.1	.22	.55	.31	.20	.065
189	7	29.8	1.13	.17	4.5	.16	4.4	.15	1.04	.51	.20	.089
193	27	54.2	1.45	.12	15.9	.50	15.9	.15	.40	.28	.23	.170
194	16	8.2	.24	.13	1.3	.05	1.3	.17	.92	.18	.09	.044
195	21	17.6	.71	.16	2.0	.09	1.2	.27	.46	.33	.17	.068
[a]196	–	--	--	.07	6.9	.34	6.9	--	--	.43	.30	--
197	5	2.0	.06	.15	.6	.56	.6	.28	.44	.16	.04	.015
[a]198	28	41.9	.93	.10	5.7	.17	5.7	.13	.54	.36	.13	.075
[a]199	10	13.2	.59	.20	5.5	.27	5.5	.21	.47	.32	.26	.112
200	30	22.3	1.80	.34	1.8	.18	1.7	.50	1.00	.80	.31	.155
201	30	21.6	1.64	.33	1.7	.28	1.3	.95	1.88	1.20	.46	.141
202	77	81.8	2.10	.10	20.8	.64	20.8	.16	.37	.33	.19	.122
203	10	14.9	.52	.15	5.9	.19	5.9	.13	.61	.18	.14	.139
204	45	34.8	1.33	.17	3.2	.13	2.4	.23	.92	.37	.15	.093
205	34	50.7	2.96	.25	4.2	.20	1.9	.24	1.08	.52	.30	.230
206	7	1.8	.08	.16	.5	.03	.5	.25	.37	.16	.06	.014
[a]207	19	12.3	1.06	.38	3.2	.39	3.2	.27	1.33	.93	.49	.095
209	16	34.8	.46	.05	3.4	.10	3.4	.12	.60	.18	.13	.048

[a]Flights for which a substantial amount of record is missing.

[b]"Total ice accumulation" represents the thickness of ice which would form on a fixed object having the same average collection efficiency as the disk.

NACA

TABLE III.— FREQUENCY OF ENCOUNTER OF VARIOUS TYPES OF METEOROLOGICAL CONDITIONS DURING THE 1948 OPERATION

Condition	No. of min condi- tion pre- vailed	Percent of total flight time	Percent of total time in contin- uous or intermittent visible moisture
Clear air	6523	61.1	--
Liquid cloud			
Continuous	209	2.0	5.0
Intermittent			
Clear air predominant	504	4.7	12.1
About one-half clear	368	3.5	8.9
Cloud predominant	325	3.0	7.8
Subtotal, liquid	1406	13.2	33.8
Mixed snow and liquid cloud			
Liquid predominant			
Continuous	180	1.7	4.3
Intermittent	384	3.6	9.2
Snow predominant			
Continuous	310	2.9	7.5
Intermittent	108	1.0	2.6
Subtotal, mixed	982	9.2	23.6
Snow			
Continuous	1122	10.5	27.0
Intermittent	228	2.1	5.5
Subtotal, snow	1350	12.6	32.5
Rain	335	3.1	8.1
Rain and snow	30	0.3	0.7
Freezing rain	13	0.1	0.3
Freezing rain and liquid cloud	41	0.4	1.0
Totals	10,680	100.0	100.0

NACA

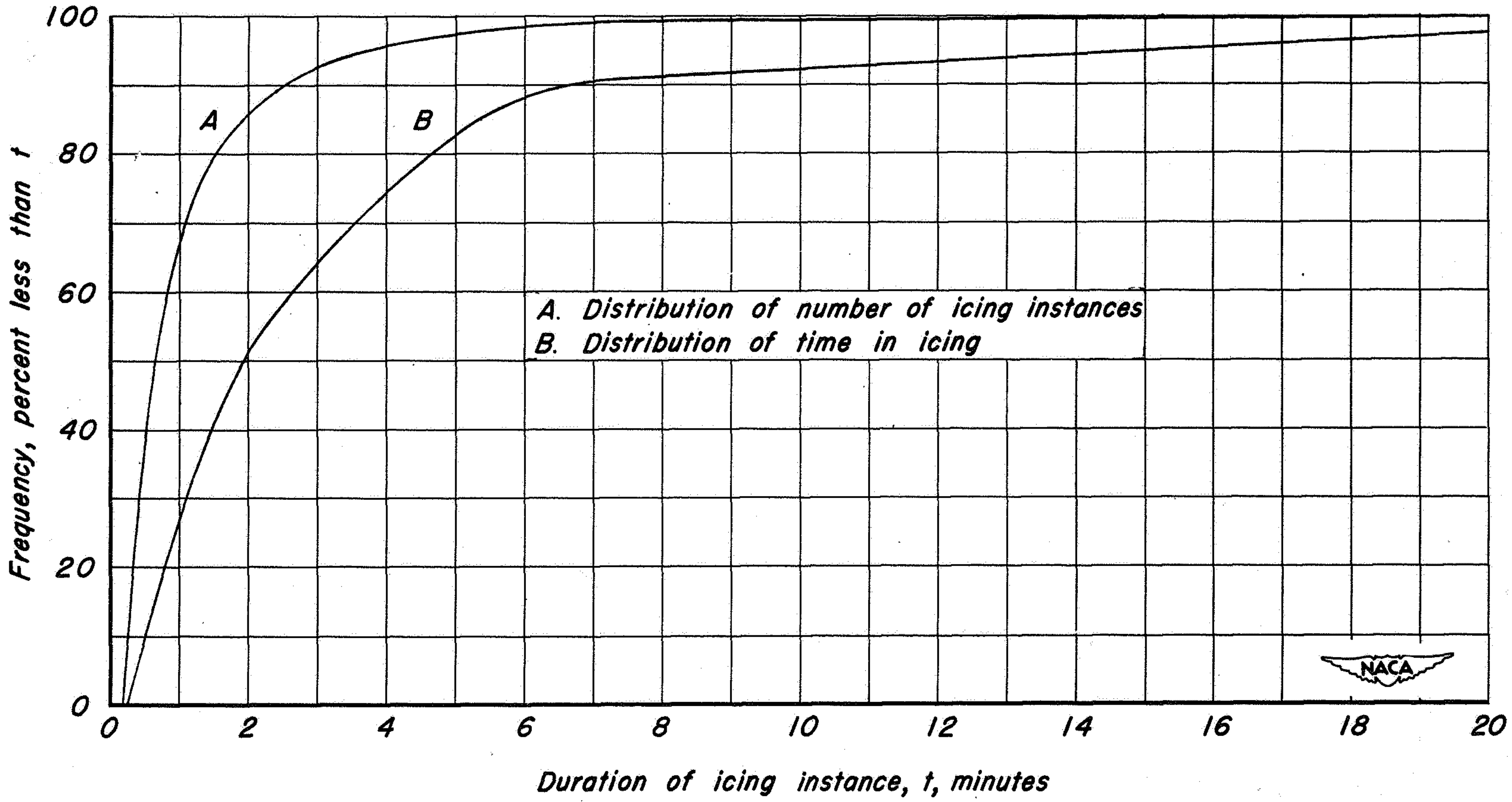

Figure 1.- Frequency curves showing the percentage of icing instances of less than a given duration and the percentage of the total flight time in icing conditions spent in instances of less than a given duration. Curves are based on 800 icing instances in 37 flights made in 1948, cumulus clouds predominated in about 2/3 of the flights.

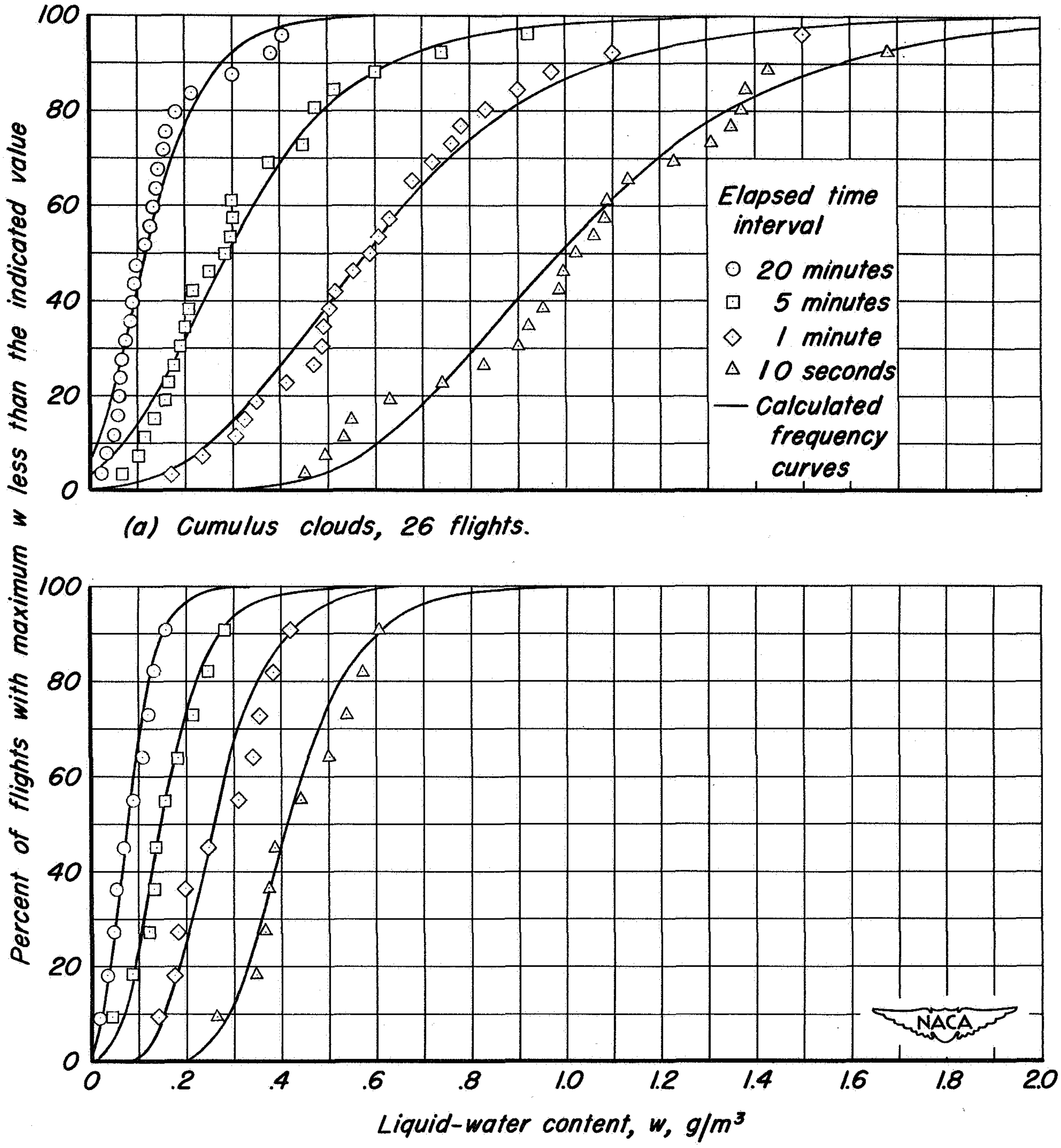

(a) Cumulus clouds, 26 flights.

(b) Layer clouds, 11 flights.

Figure 2.- Frequency distributions of maximum liquid-water content per flight averaged over various elapsed time intervals for layer clouds and cumulus clouds. Data points represent observed distributions, curves are calculated by method of reference 5. Average flight speed 180 miles per hour.

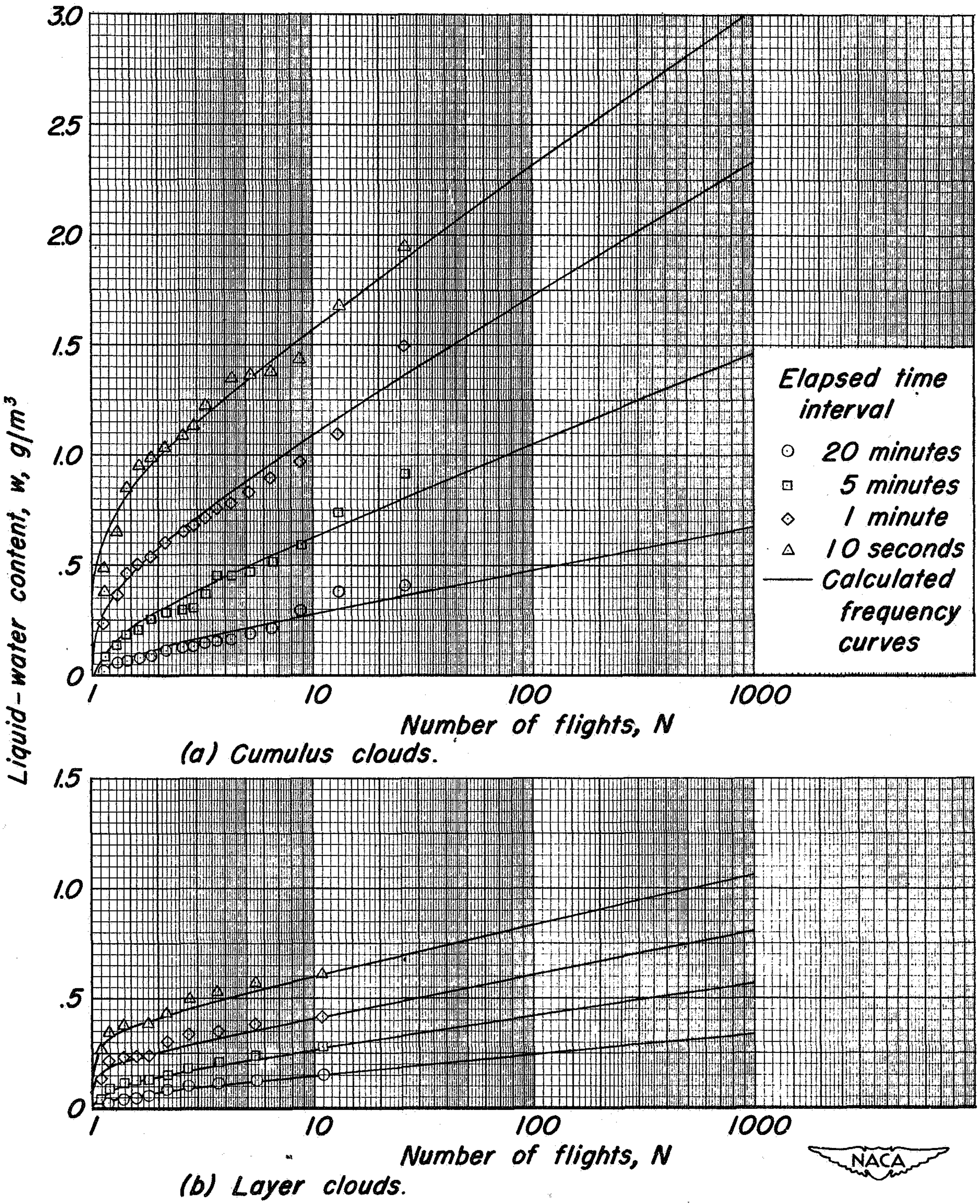

Figure 3.- Probable maximum values of liquid-water content averaged over various time intervals as a function of number of flights in layer clouds and cumulus clouds. Average flight speed, 180 miles per hour.

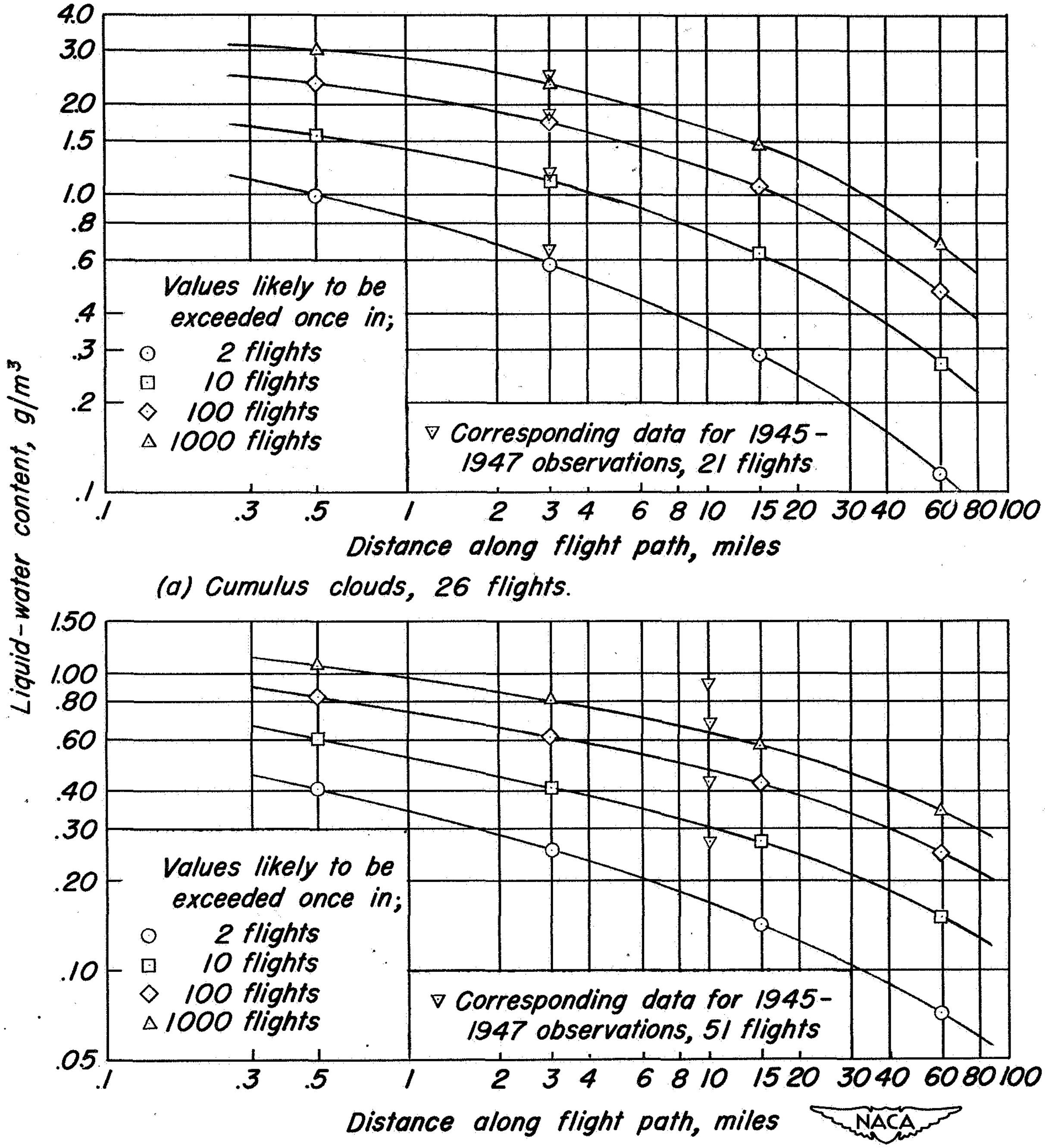

(a) Cumulus clouds, 26 flights.

(b) Layer clouds, 11 flights.

Figure 4.– Maximum liquid-water content averaged over various distances along flight path. Average flight speed, 180 miles per hour.

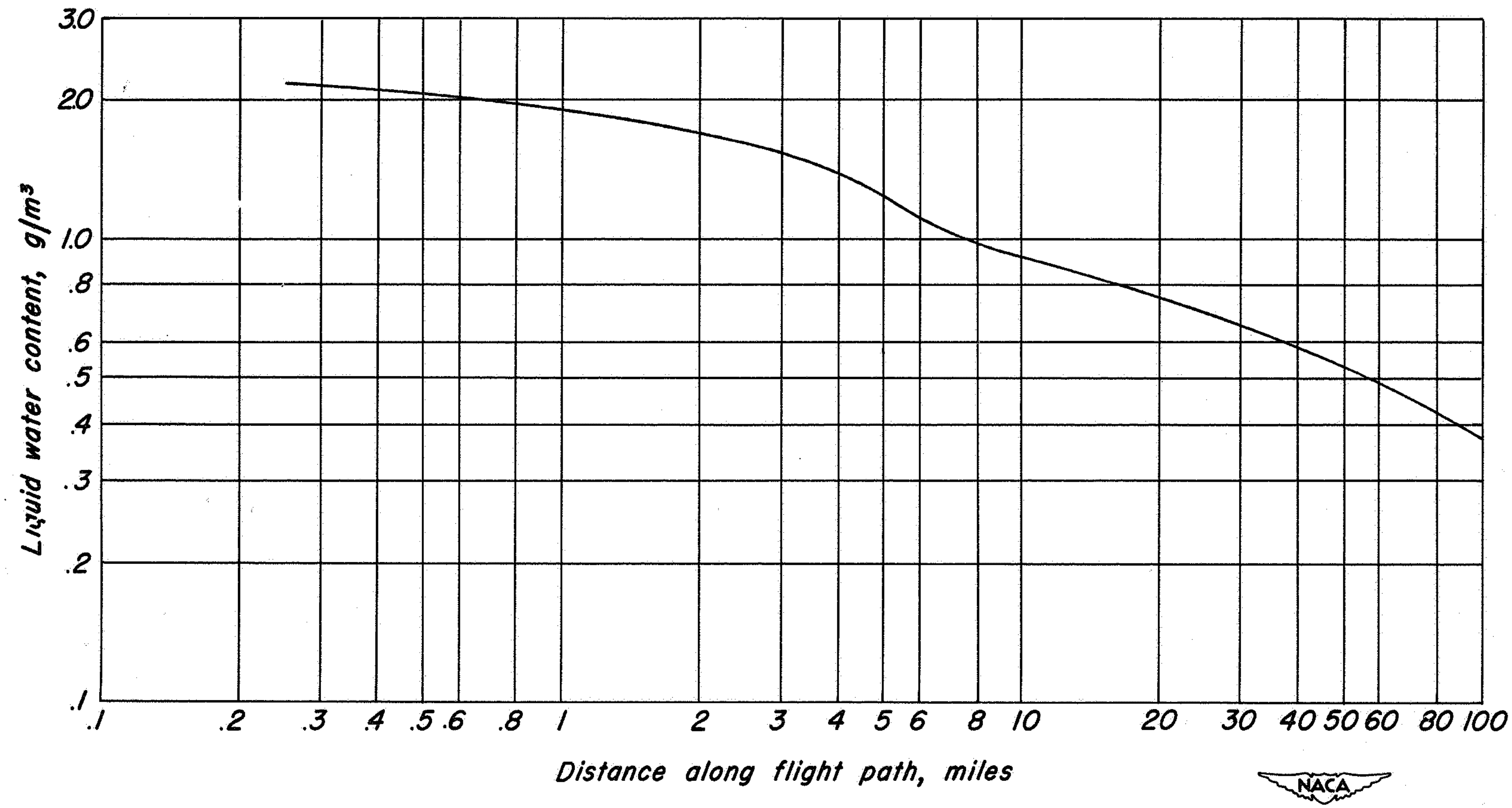

Figure 5.– Estimated maximum values of average liquid-water content to be expected in 1000 flights encountering icing, assuming 5 percent of flights encounter cumulus clouds.

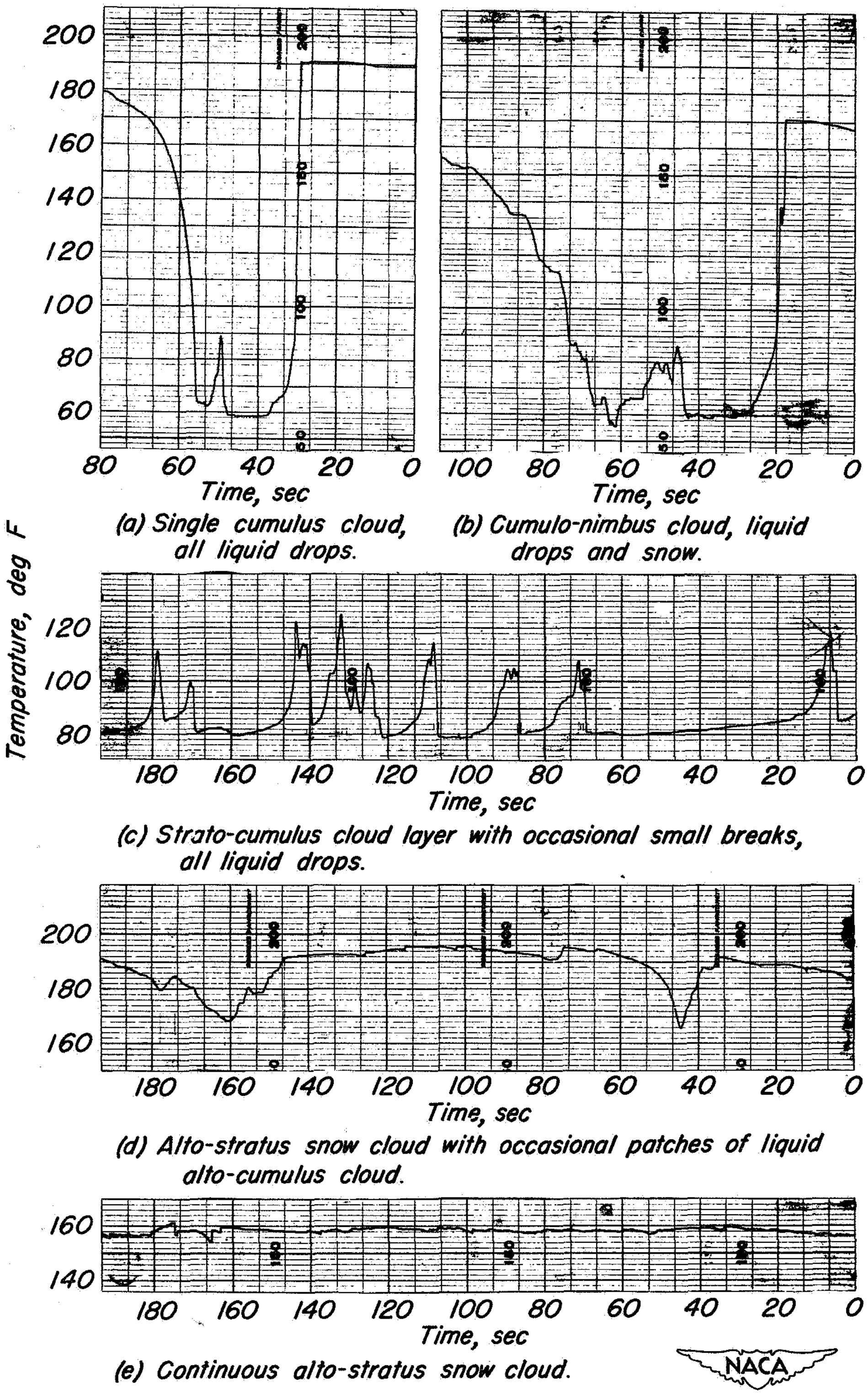

Figure 6.-Typical cloud-indicator records showing response to various cloud types.

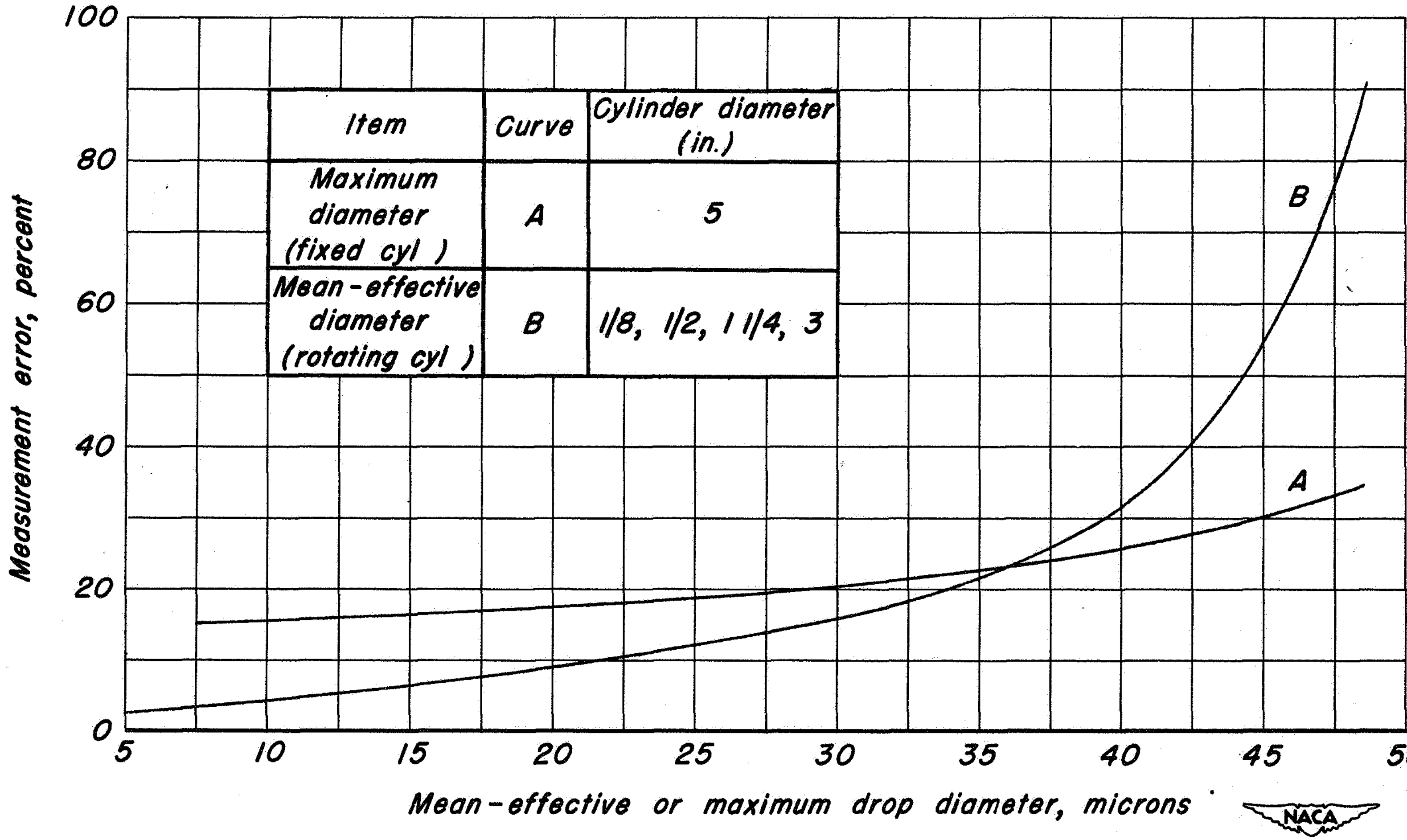

Figure 7.-Calculated error in the measurement of mean-effective drop diameter with four rotating cylinders, and maximum drop diameter with one nonrotating cylinder. Calculations based on assumption of errors of ± 5% in determining the weight of ice accretions on the rotating cylinders, and + 5° in the determination of the angle of water impingement (θ_m) on the nonrotating cylinder.

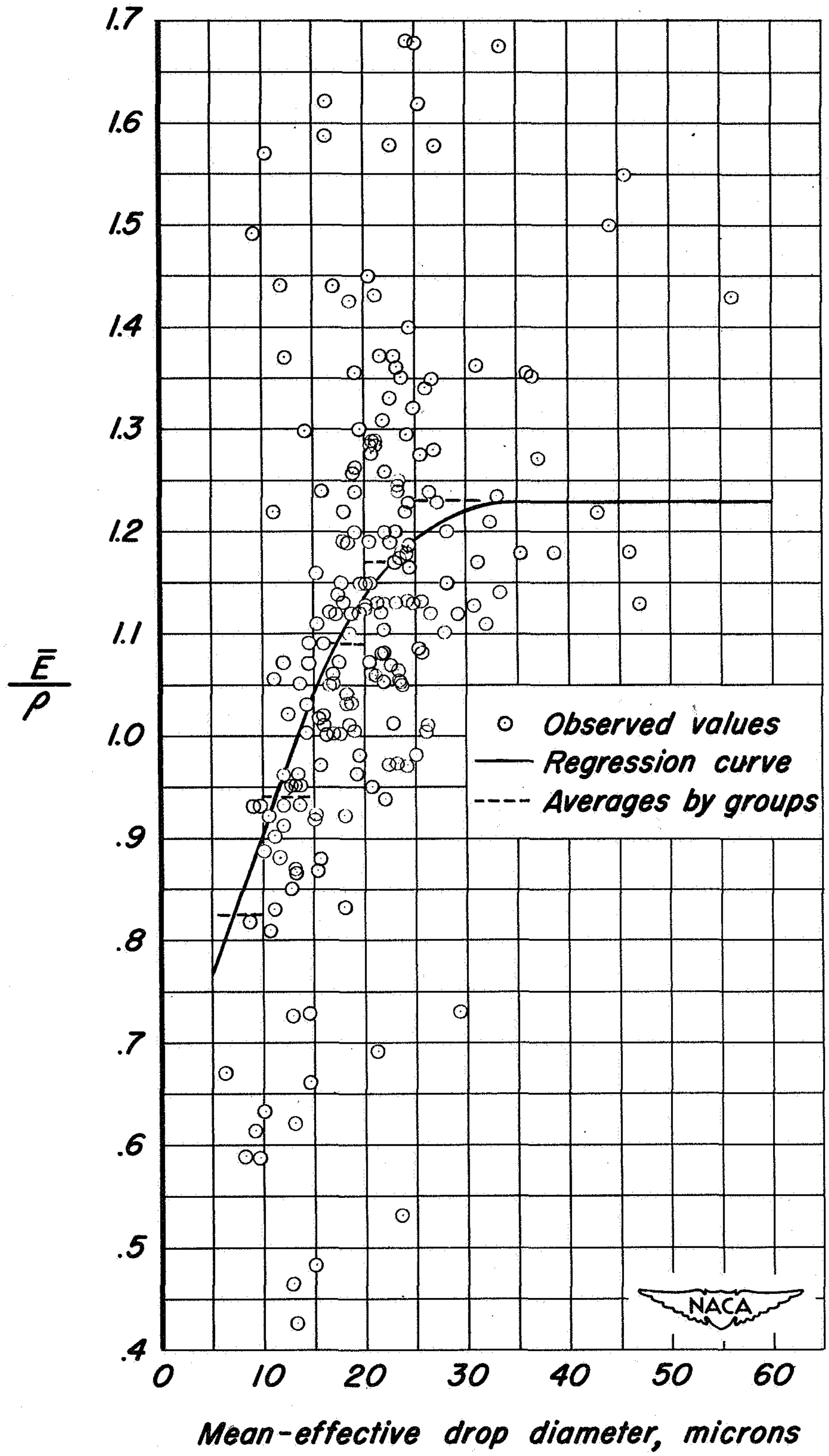

Figure 8.– Relation between drop diameter and ratio of collection efficiency of disk to density of ice.

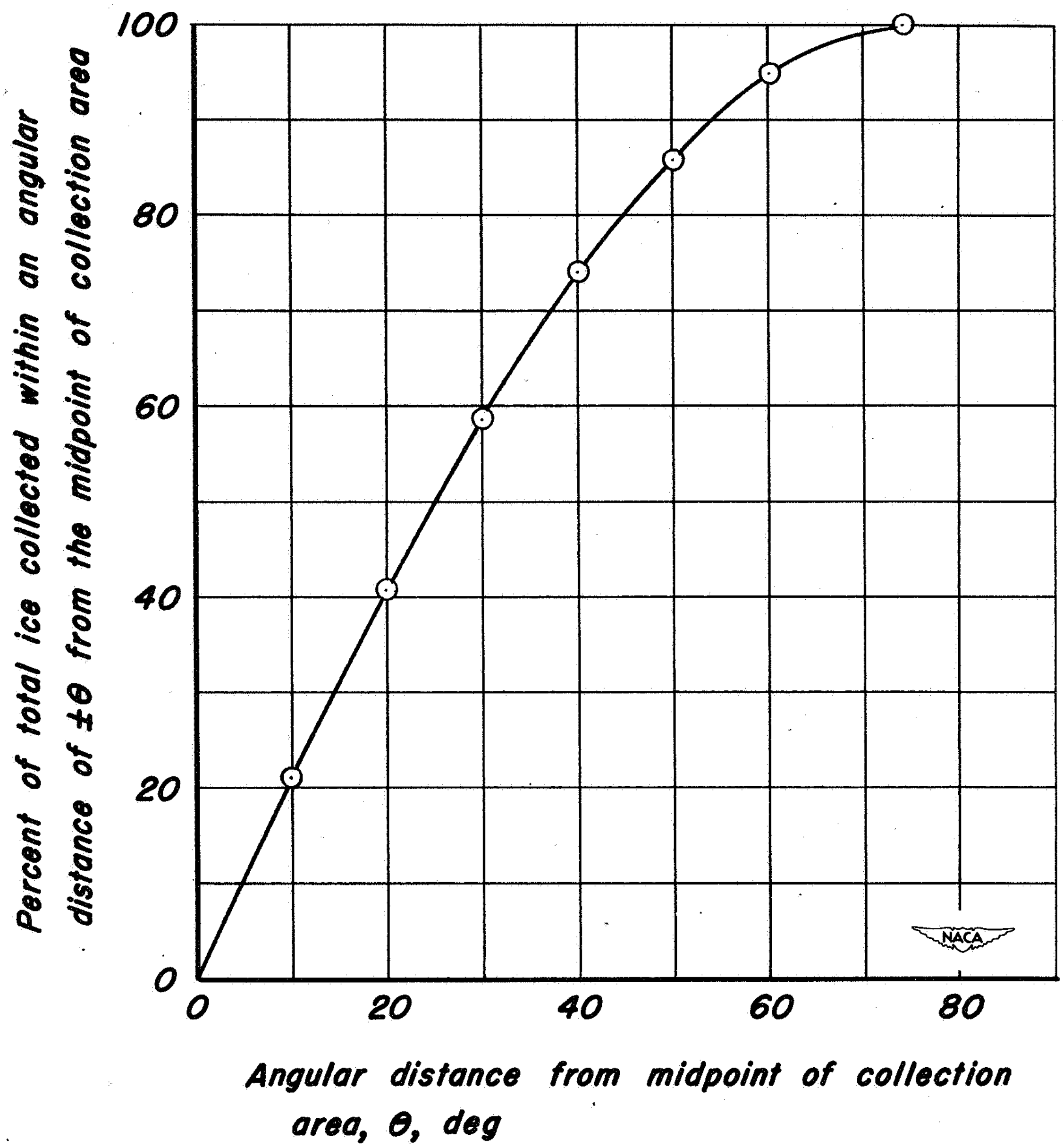

Figure 9.– Distribution of ice collection on rotating disk.

Note: x and y are coordinates as measured on recorder film.

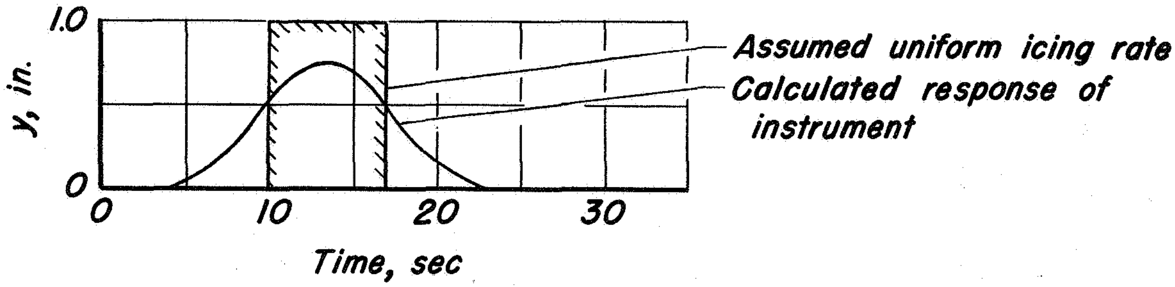

(a) Response to 7 seconds of flight in uniform cloud.

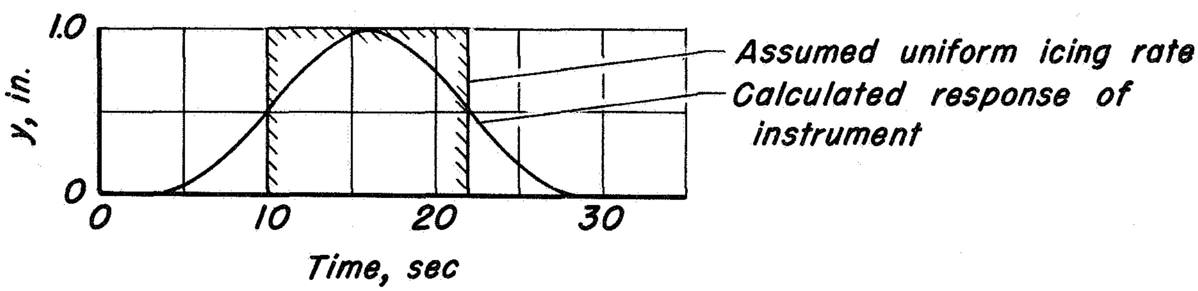

(b) Response to 12 seconds of flight in uniform cloud.

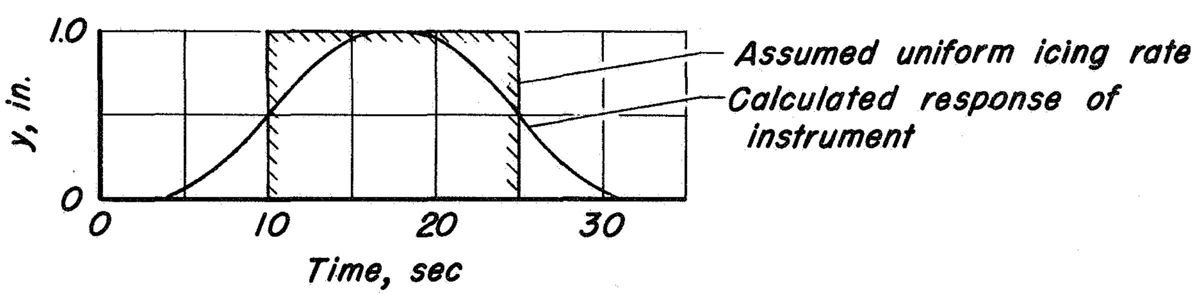

(c) Response to 15 seconds of flight in uniform cloud.

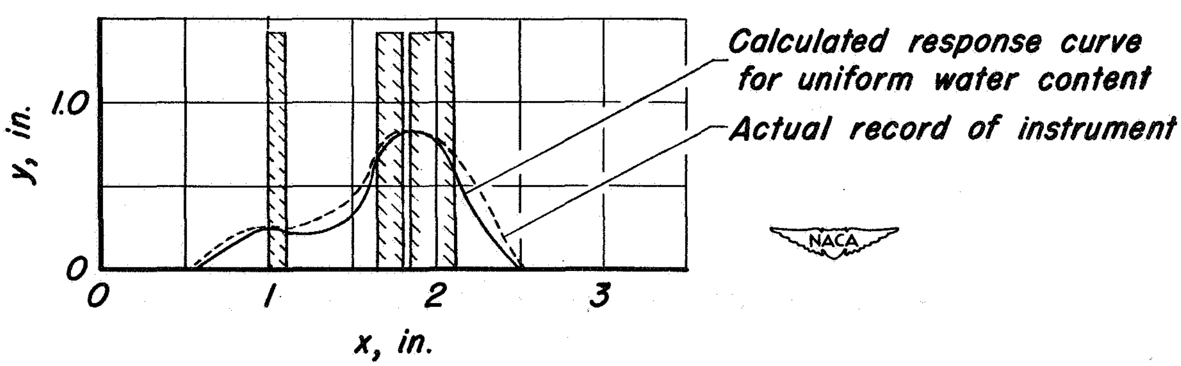

(d) Response to actual cloud.

Figure 10.- Illustrative icing-rate meter response curves.

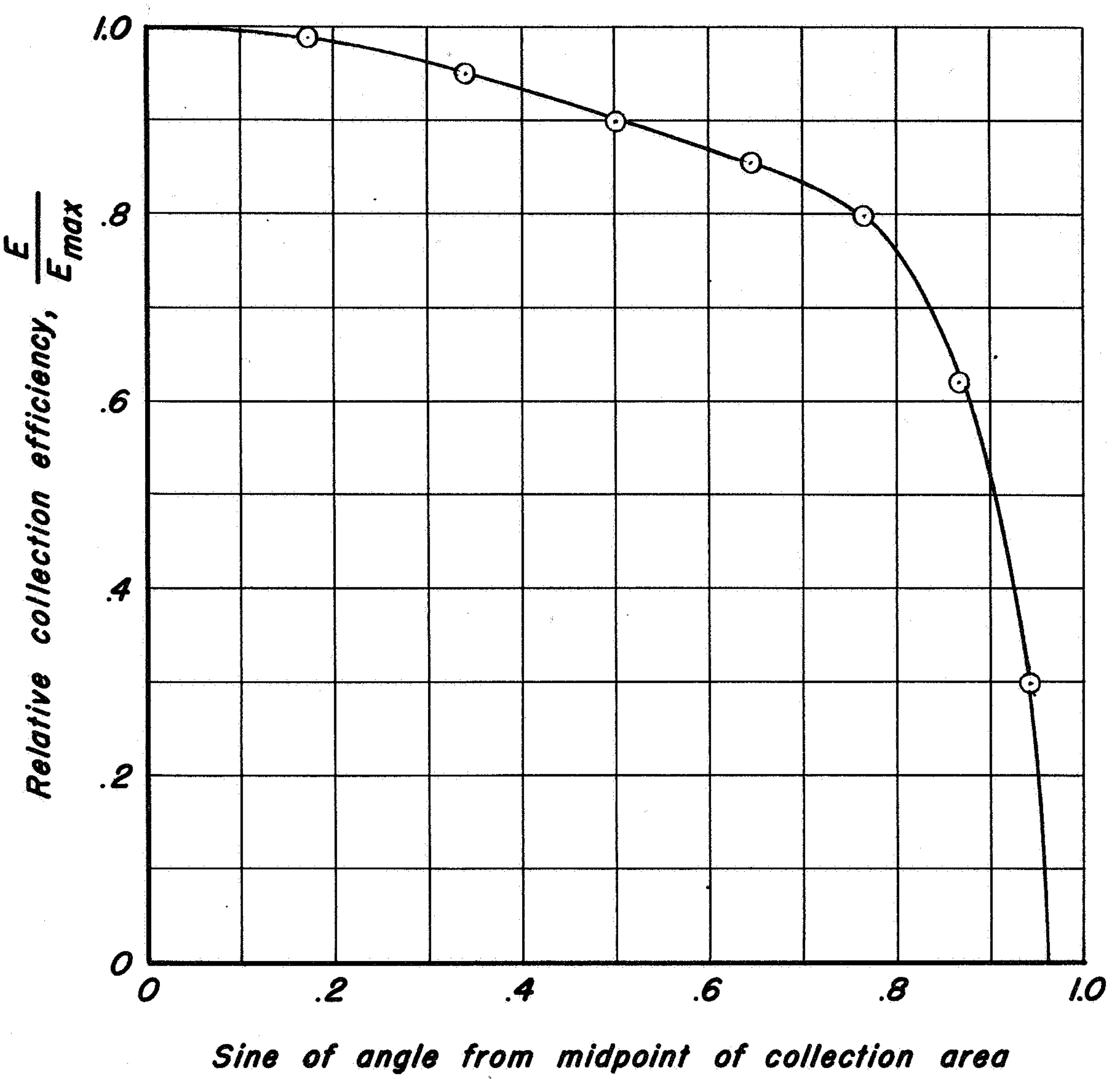

Figure 11.– Collection efficiency, E, along edge of disk referred to collection efficiency, E_{max}, at midpoint.